https://doi.org/10.5194/egusphere-2026-3848
Preprint. Discussion started: 21 July 2026

Quantifying parametric uncertainty in future food demand in GCAM

Brian C. O'Neill,[1,2] Kanishka Narayan,[1] Stephanie T. Morris [1]

[1] Joint Global Change Research Institute, Pacific Northwest National Laboratory, College Park, MD, USA
[2] Center for Global Sustainability, University of Maryland, College Park, MD, USA

Correspondence to: Brian O'Neill (brian.oneill@pnnl.gov)

Abstract. Projecting food demand is important for understanding the future of land, water, and energy in the integrated human-Earth system and also has implications for health and human well-being. Uncertainty in demand has many drivers, including model structure, technological change, socio-economic development, trade, and policies. An under-studied driver is the uncertainty in model parameters estimated on historical data. We use the Global Change Analysis Model (GCAM), an integrated model of land, water, energy, and economy interactions, to investigate the parametric uncertainty in projected food demand. We modify GCAM's demand functions to better represent regional variation in consumption patterns, disaggregate consumption within regions across income deciles, and re-estimate uncertain parameters. To more efficiently characterize uncertainty, we use the demand functions as an emulator of the full food system in the more complex model and project a large ensemble of demand for staples and non-staples in a GCAM reference scenario. We find that parametric uncertainty in demand, as well as in the response of demand to price changes, is a substantial source of uncertainty in future outcomes and is especially large in low-income deciles. Using scenario discovery techniques, we identify five sets of parameters that effectively span the range of uncertainty across regions and deciles in both demand and its response to price changes. These parameter sets allow GCAM users to capture parametric uncertainty in a small number of scenarios. This uncertainty in demand can substantially affect uncertainty in cropland, water withdrawals, and biomass production in some regions.

1. Introduction

Food consumption is an important factor in health and well-being, and the magnitude of demand for food and the composition of diets also interacts with changes to land use and the energy, water, and Earth systems. However, there is large uncertainty around the evolution of future food demand (Flies et al., 2018; Valin et al., 2014; van Dijk & Meijerink, 2014; van Dijk et al., 2021; von Lampe et al., 2014; Yu et al., 2004). Uncertainty in projections of food demand – whether at the subnational, national, or global level – comes from multiple sources. These include the mathematical structure of demand models, the calibration and parameterization of the models, the socioeconomic scenarios that drive them, aspects of food supply such as technological change, and the connections between food systems and land, energy, water, and trade in

https://doi.org/10.5194/egusphere-2026-3848
Preprint. Discussion started: 21 July 2026

human-Earth system models. One such model, the Global Change Analysis Model (GCAM; Calvin, 2019), underlies the analysis in this paper. It is an integrated model of land, water, energy, and economy interactions, and includes a food system that is subject to all of the uncertainties just described.

Demand system structure – the relationship between food demand and its drivers, including income, prices, and other expenditures – is not known with certainty and has been modeled in multiple ways. Systematic comparisons across alternative approaches show significant differences in projections of food expenditures (Yu et al., 2004) and clear distinctions between simpler systems and (preferred) more complex models that allow for income elasticities to change with income (Cranfield et al., 2003). The GCAM food demand structure (Edmonds et al., 2017; Narayan et al., 2021) models demand for two food commodities, staples (grains, roots and tubers) and non-staples (all other non-alcohol food consumption), with income and price elasticities that vary with income. Bijl et al. (2017) calibrate a physically-based demand model, which uses a log-linear relationship between food demand and income, body weight, physical activity, and food waste for six food commodity groups.

Within a given model structure, uncertainty in key parameters, particularly income and price elasticities, can generate large differences in projected food demand (Valin et al., 2014; von Lampe et al., 2014). Elasticities also strongly depend on the socio-demographics of a region (Roche et al., 2025), which can change substantially over time. Yet full consideration of parametric uncertainty is rare. Estimation of parameters for the original version of the current GCAM food demand model (Edmonds et al., 2017) included the joint uncertainty across nine demand parameters, but we are not aware of other similarly comprehensive treatments. Parameter estimation can be difficult due to limited data and differences in preferences across regions or groups within a region. Demand elasticities are frequently estimated from either household survey data (Andreyeva et al., 2010; Kumar et al., 2011; Tiffin & Tiffin, 1999) or country-level data (Muhammad et al., 2011), potentially limiting the applicability of results to other regions or consumer types.

One of the largest drivers of uncertainty in demand projections is the underlying scenarios of socioeconomic change (Valin et al., 2014; van Dijk et al., 2021; von Lampe et al., 2014). Scenario components that influence demand include regional population and GDP per capita, income distribution, age structure, rural/urban status, rates of technological change, trade (Zhao et al., 2022), and dietary preferences (Bodirsky et al., 2015), among others. Income distribution is of particular importance to total food demand, as the share of household expenditures on food decreases as incomes increase; ignoring heterogeneity in consumers' income levels will distort aggregate outcomes (Blundell & Stoker, 2005; Cirera & Masset, 2010; Denton & Mountain, 2001, 2011; Park et al., 1996). Understanding the demand profile for consumers at different income levels is also essential for projecting food security measures (Li et al., 2021; Pinstrup-Andersen & Caicedo, 1978; Ren et al., 2018).

https://doi.org/10.5194/egusphere-2026-3848
Preprint. Discussion started: 21 July 2026

Interactions between the food system and land, water, energy, and Earth systems also drive uncertainty. Integrated human-Earth system models (such as GCAM) account for such interactions and are frequently used to understand longer-term evolution of food demand (Nelson et al., 2014; Valin et al., 2014; von Lampe et al., 2014). They are increasingly accounting for income distribution within regions both to improve the projections of aggregate demand and to explore outcomes for different income groups within regions (Bijl et al., 2017; Sampedro et al., 2022; Sampedro et al., 2024; Zhang et al., 2025).

These multiple sources of uncertainty give rise to a methodological challenge around how to efficiently explore the range of possible futures and identify a small number of scenarios that effectively captures uncertainty in metrics of interest. Exploring the food demand uncertainty space potentially requires a large number of runs (Reilly & Willenbockel, 2010) with prohibitive computational expense. One approach to this task has been to use emulators, simple models that are trained on more complex and computationally demanding models, and scenario discovery techniques to identify outcomes of interest that can then be the focus of the development of a small number of scenarios with the complex models (Lamontagne et al., 2018). Recently, the first emulators of human-Earth system models have been developed (Holmes et al., 2024; Xiong et al., 2025).

In this paper, we quantify parametric uncertainty in food demand using GCAM and an emulator of its food system. To emulate food demand we use *ambrosia* (Narayan et al., 2021), a separate model that we developed to help design – and which therefore now replicates – the GCAM food demand functions. We begin by estimating the joint uncertainty in demand function parameters given historical observations of food consumption, income, and prices. We then use the *ambrosia* model, combined with this uncertainty distribution across parameters, to produce a large ensemble (10k simulations) of food demand projections for GCAM's 32 global regions for the period 2021-2100. We then use this ensemble to identify a small number (4) of alternative parameter sets that effectively spans uncertainty in future food demand and its response to price changes. These parameter sets can be employed by GCAM users to introduce uncertainty in food demand in scenario-based analyses.

This approach assumes that the large ensemble of demand projections generated with ambrosia is a reasonable representation of the uncertainty in the demand that GCAM would produce if it were used to generate the same ensemble. This is not necessarily the case, given that ambrosia takes prices as exogenous while GCAM includes the potential for alternative demand parameters to lead to price changes that would feed back on demand. An important element of the analysis is therefore to evaluate how well ambrosia emulates demand behavior in GCAM in order to validate the approach.

In the next section we describe the methods used in the analysis, followed by a description of results and a concluding discussion. Supplementary Material provides a substantial amount of additional information supporting the main analysis.

https://doi.org/10.5194/egusphere-2026-3848
Preprint. Discussion started: 21 July 2026

2. Methods and data

We first describe the GCAM model, its food demand module, and how we modify its functional form and introduce income deciles within regional populations. We next describe the re-estimation of food demand parameters, including data, methodology, and basic results. Finally, we describe how we use GCAM and ambrosia together, along with uncertain parameter estimations, to characterize uncertainty in demand and identify alternative sets of parameters representing that uncertainty.

2.1. GCAM model and modifications

The Global Change Analysis Model (GCAM) is a state-of-the-art MultiSector Dynamics model that represents the interactions between the land system, the economy, water systems, food systems and energy systems among 32 geographical regions (Calvin et al. 2019, Binsted et al. 2021). For this paper, we modify the food demand component of GCAM v8.6 (JGCRI, 2025) in two main ways: we modify the staples food demand function to better represent regional variation in demand patterns, and we disaggregate food demand within each region into 10 equal-population groups differentiated by income.

The GCAM food demand model expresses demand for two categories of food goods – staples and non-staples – as a function of per capita income, prices of each good, and a set of nine parameters (Edmonds et al., 2017). Three parameters control the income elasticity of demand for each good, which varies with income level. Another three determine the price elasticities of each good, which also vary with income. The final three are scale parameters. The model captures a number of stylized facts about food demand (Fig. 1): as income increases (holding prices constant), staples demand first increases, then peaks and declines, while non-staples demand increases monotonically, implying a shift in demand from staples to non-staples; at higher incomes, composition stabilizes and total food demand saturates. Responses to price changes include both substitution and income effects, with staples and non-staples acting as substitutes at lower incomes and complements at higher incomes.

https://doi.org/10.5194/egusphere-2026-3848
Preprint. Discussion started: 21 July 2026

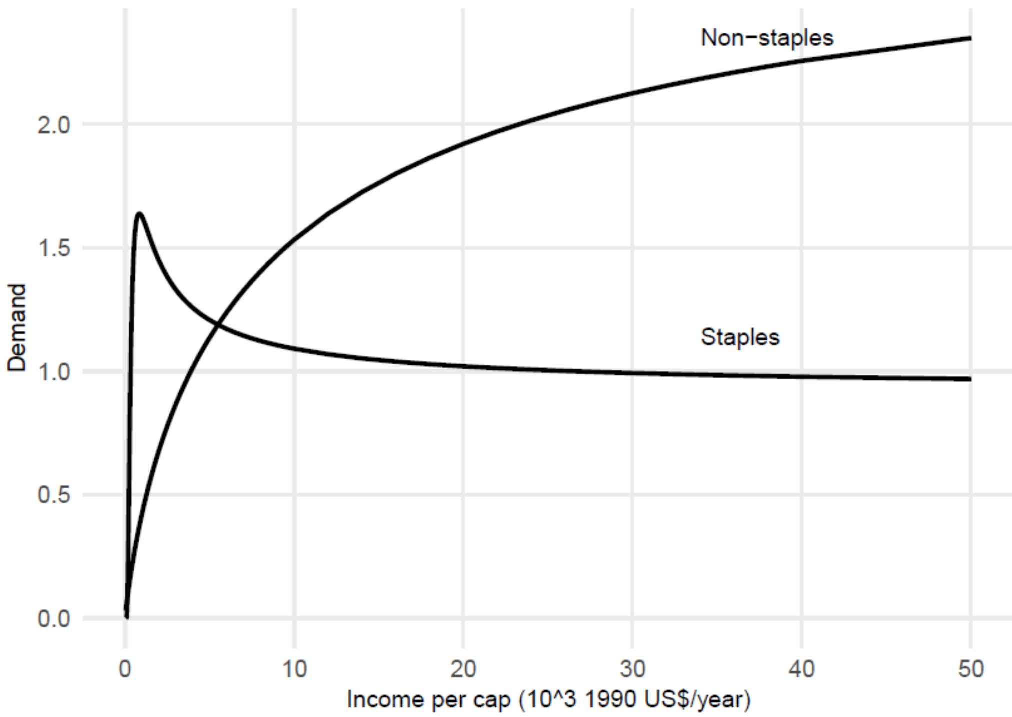

Figure 1: Illustrative staples and non-staples demand as a function of per capita income, assuming constant prices at typical values ($P_s = 0.05$, $P_n = 0.25$), representative global parameter values (maximum likelihood, as derived in section 3.2), and zero fixed effects.

We have modified the GCAM v8.6 demand system in two ways: by adding regional fixed effects for staples and minimum demand thresholds (see supplementary text for details). Regional staples' fixed effects were motivated by the fact that, while the original demand functions captured well the qualitative behavior of staples demand with rising income, the fit to observations left room for improvement (discussed in the next section) and was indicative of regional variation. Minimum demand thresholds were added because the functional form of the model does not guarantee realistic behavior at very low incomes (and with fixed effects, staples demand can even be negative at or near zero income). This is especially important given our extension of the consumer representation to include sub-populations defined by deciles of income, meaning that consumers with much lower income than the regional average (the original application) are represented.

In addition to changes in food demand functions, we introduced income deciles that have the same food demand functions within a given region but respond differently according to their income levels. For example, the lowest income consumers spend a larger portion of their budget on food, and patterns of staples and non-staples demand shift as described above. Income distributions evolve over time based on exogenous projections from Narayan et al. (2023), who produced decile-scale income distribution projections to 2100.

https://doi.org/10.5194/egusphere-2026-3848
Preprint. Discussion started: 21 July 2026

Food demand is calibrated to observed data (FAO) in the base year (2021) at the regional level, given the lack of such data at the level of income deciles. Consumption at the decile level is initialized using the demand functions and the prevailing income levels, and the regional average per capita consumption is calculated. The difference from the observed per capita consumption is applied as an additive bias term equally to each decile, and this bias is carried forward in all future years.

2.2. Data collection and parameter estimation

Parameter estimation was carried out based on data on food consumption by commodity from the FAO food balance sheets from 1971-2017. We also compiled producer commodity prices for several food commodities for that same time period. Commodity prices were aggregated to staple and non-staple prices per calorie based on food consumption and caloric content at the GCAM region level. Basing this aggregation on consumption rather than production controlled for trade and implied prices that better approximate consumer prices.

Given our interest not only in best estimates of parameters but their uncertainty distributions, we carry out the estimation using a Bayesian Markov Chain Monte Carlo (MCMC) approach with the Metropolis-Hastings algorithm, as in Edmonds et al. (2017). Details of the MCMC approach are described in the supplementary text. In broad terms, the method begins with assumptions about the prior uncertainty distributions over parameters and then updates those assumptions based on a comparison of predicted demand to observations. The comparison takes the form of the calculation of the likelihood of the observations conditional on a candidate set of parameter values. Successive candidate parameter sets are generated based on the ratio of the likelihood of a proposed set to that of the current set, which guides the chain of proposed sets toward a stable, posterior distribution of the joint uncertainty across parameters. We calculate joint distributions for 41 parameters (9 global parameters and 32 regional fixed effects).

We assume uniform priors for all parameters, constrained as described in Table C1 based on physical and economic plausibility. We run the MCMC routine until about 50 thousand samples of the posterior have been generated and then choose a random sub-sample of 10 thousand of these for the calculations in the rest of the paper.

Figure 2 shows the posteriors for the nine global parameters along with their maximum likelihood (ML) estimates (see Fig. B1 for distributions for 32 regional fixed effects). The ML parameters provide a good fit to the observations (Figs. B3 and B4, Table C2), with high correlation (>= 0.9 for staples and non-staples) and relatively low absolute and percentage errors. Bias in total food consumption is very small, although there is a slight composition bias with under-prediction of staples demand and over-prediction of non-staples. This fit is a substantial improvement over the ML parameters derived in Edmonds et al. (2017), based on a demand model without fixed effects in staples demand. Those parameters produced a

https://doi.org/10.5194/egusphere-2026-3848
Preprint. Discussion started: 21 July 2026

correlation with observations of staples consumption of 0.53 and mean errors (RMSE, MAE, MAPE) for staples about twice as large as the new model (Table C2).

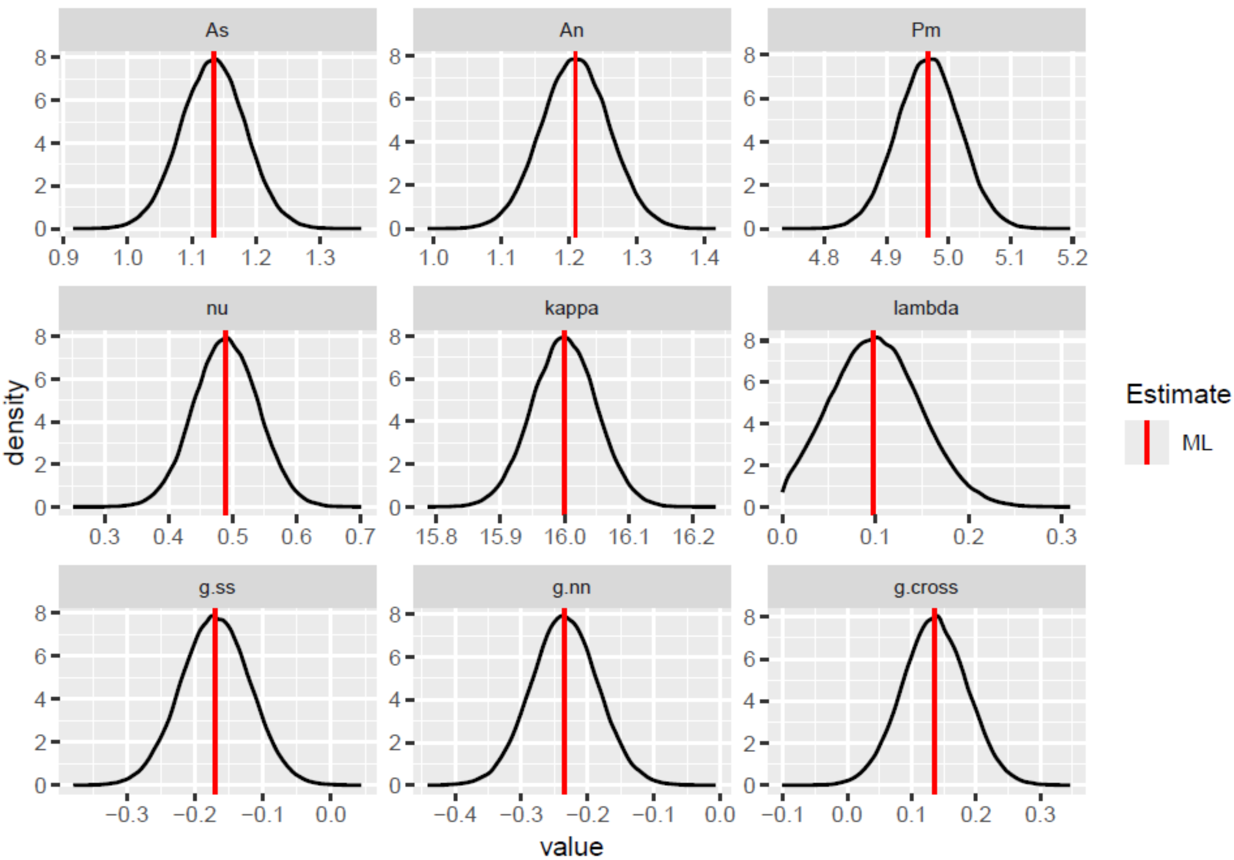

Figure 2: Posterior distributions of global food demand parameters, with maximum likelihood (ML) values marked by the red vertical line. Posteriors of regional fixed effect parameters are provided in Fig. B1. See supplementary text for parameter definitions.

The ML parameters imply income and price elasticities that have expected patterns (Fig. 3) given the stylized facts that the demand functions represent. Income elasticities are positive at the lowest income levels for staples before turning negative, and positive over all incomes for non-staples. Own-price elasticities are negative for both food types and slightly larger in magnitude for non-staples. Cross-price elasticities are positive for both food types, indicating substitution behavior, except for staples at the lowest income levels where the income effect dominates and higher non-staples prices lead to a decrease in consumption of both goods.

https://doi.org/10.5194/egusphere-2026-3848
Preprint. Discussion started: 21 July 2026

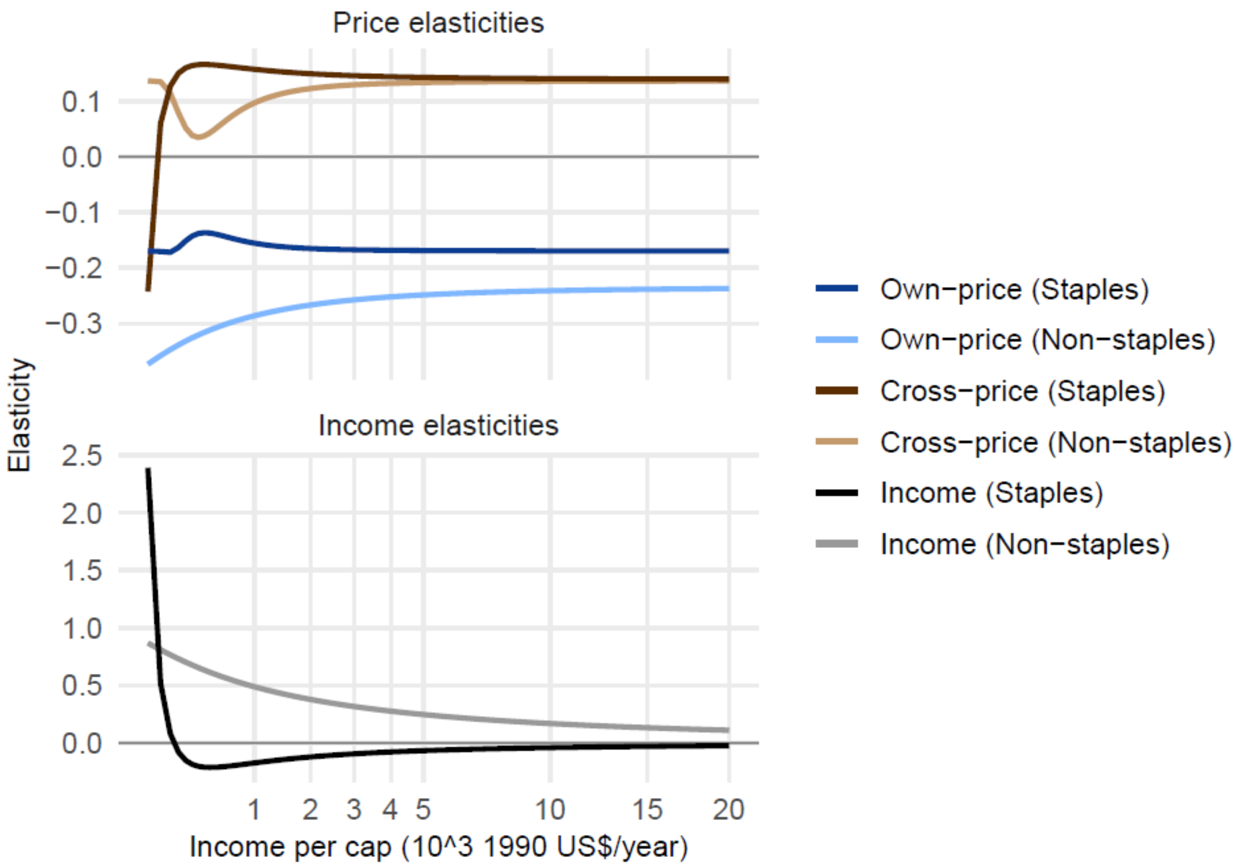

Figure 3: Implied price and income elasticities of demand as a function of income for the maximum likelihood parameter values, assuming constant prices at typical values (Ps = 0.05, Pn = 0.25). The x-axis is shown on a square-root scale to make results at low incomes clearer. Figure B2 shows a comparison of these results to previous model versions.

190 ### 2.3. *Ambrosia* ensembles and parameter identification for scenarios

The joint posterior distributions characterizing parameter uncertainty were used, along with ambrosia, to generate corresponding distributions of emulated demand for staples and non-staples for all GCAM regions for two different scenarios of food prices and per capita income (including its distribution over deciles). These income and price scenarios were taken from two GCAM scenarios. The first is from the GCAM Reference scenario, which assumes that socio-economic drivers (population and GDP growth) and rates of technological change follow middle of the road pathways based on SSP2, and assumes no explicit policy or institutional changes. The second scenario is taken from a GCAM High Price Conditions (HPC) scenario in which price multipliers are implemented in GCAM to force staples and non-staples prices to approximately double over the rest of the century while all other assumptions are the same as in the Reference.

https://doi.org/10.5194/egusphere-2026-3848
Preprint. Discussion started: 21 July 2026

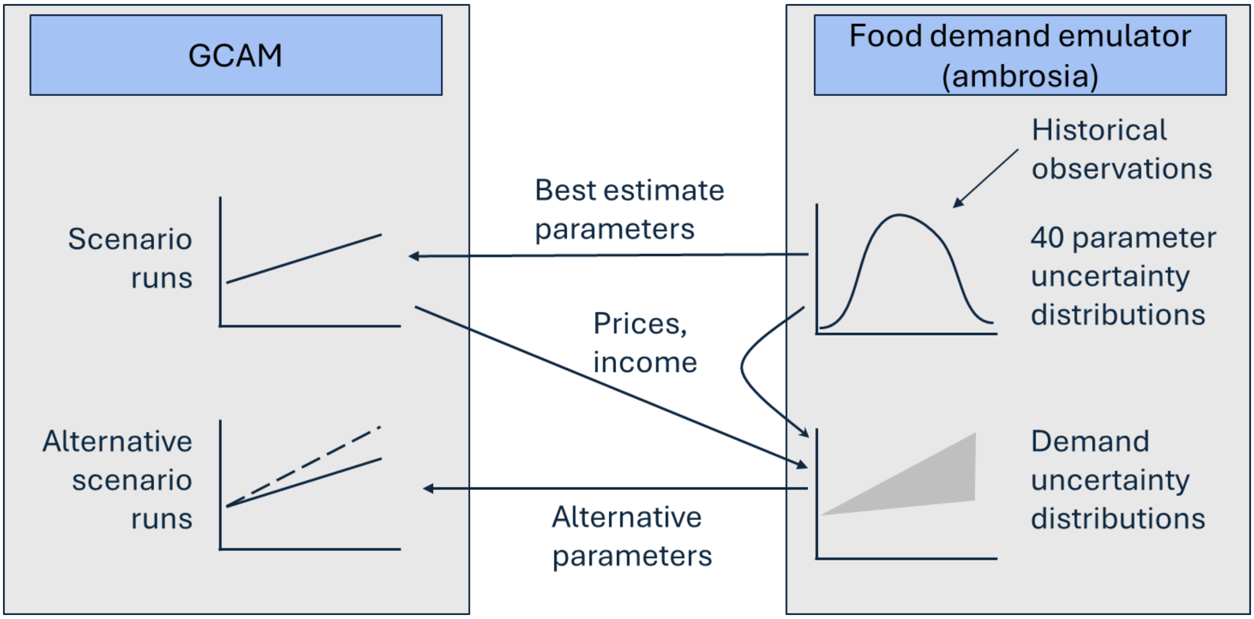

Figure 4: Simplified outline of experimental design in this study. GCAM is used to run initial scenarios using maximum likelihood parameter values determined by ambrosia, and then to run additional scenarios based on alternative parameter sets that are designed to capture demand uncertainty reflected in ambrosia ensembles. Ambrosia is used to derive parameter uncertainty distributions and projected demand uncertainty distributions from which parameter sets are identified.

This step generated 10 thousand demand pathways, differing only in their food demand parameters, for each of the two scenarios. In each pathway, ambrosia was calibrated to observations in the base year in the same manner as GCAM, deriving an additive regional bias term such that regional per capita demand matches observed consumption and carrying that term forward to all projection years.

A third set of 10 thousand pathways was produced by subtracting the first two sets in order to derive an uncertainty distribution of the difference in demand due to the price change between the HPC and Reference scenarios. Finally, three additional sets of 10 thousand pathways each were produced for the Reference scenario, HPC scenario, and their difference in order to inform a decomposition of uncertainty. The parameters were categorized into those that affect the response to income (nu, kappa, and lambda in Fig. 2 and the supplementary text) or to price changes (g.ss, g.nn, g.cross) and those that affect scale (A_s, A_n, P_m, and regional fixed effects). Ensembles were generated in which parameters in each of these categories were varied over their full posterior distribution while parameters in the other two categories were held fixed at

https://doi.org/10.5194/egusphere-2026-3848
Preprint. Discussion started: 21 July 2026

their ML values. Results allow for the decomposition of uncertainty in absolute demand in either the Reference or HPC scenarios, as well as in the demand response to the increased prices in the HPC scenario.

These ensembles of ambrosia results also provided the basis for identifying a small number of parameter sets that could be used in GCAM to effectively span the uncertainty in absolute demand (high or low demand, HD/LD) or in the response of demand to price changes (high or low price response, HPR/LPR). In principle, the parameter sets that best represent these features depend on income level, food type, prices, and region, so it is not clear in advance whether a small set exists that can span these results over a wide range of conditions. We searched for these sets by maximizing the number of regions and time steps for which a given parameter set produced projected total food demand that was either especially low or high, while also producing a relatively low or high demand response to price changes. The details of this process are described in the supplementary text.

Goodness of fit metrics show that the four alternative parameter sets (HD–HPR, HD–LPR, LD–HPR, LD–LPR) represent plausible but less accurate outcomes relative to observations (Figs. B3 and B4, Table C2), consistent with the role of these parameter sets in bracketing uncertainty rather than optimizing fit. Across these cases, error measures (RMSE, MAE, and MAPE) are higher than in the ML case, particularly for non-staples, where MAPE is roughly 19–27%. This reflects a greater sensitivity of non-staples demand to parameter variation. However, correlations with observations are relatively high for staples and non-staples (generally 0.7–0.9), indicating that the alternative parameter sets still capture broad patterns of variation in demand. Performance for total demand is more uneven, with low demand cases indicating weaker ability to reproduce variations (correlations of ~0.35–0.50).

3. Results

We first discuss results describing the magnitude of parametric uncertainty in projected food demand across regions, income deciles, and food types. We also discuss the magnitude of uncertainty in the demand response to price changes, and the drivers of both of these types of uncertainty. We then turn to the identification of four alternative parameter sets and their use in GCAM to span uncertainty, before looking at the consequences of this uncertainty for outcomes in other sectors.

3.1. Emulated uncertainty ranges in future food demand

The large ensemble of demand simulations produced with the emulator demonstrates that, when driven by income and prices from the GCAM reference scenario, parametric uncertainty produces uncertainty in food demand that varies by region, level of aggregation, and food type. Figure 5 illustrates this range. Uncertainty is relatively small in US regional demand, particularly for staples, given the stable pattern of per capita demand at the region's income level. Even so, it can be substantially larger for individual deciles, particularly for non-staples. Uncertainty is larger for China for both food types,

https://doi.org/10.5194/egusphere-2026-3848
Preprint. Discussion started: 21 July 2026

and it varies over deciles. The pattern of high near-term uncertainty in staples demand for decile 1, followed by uncertainty that declines and then increases again, reflects the fact that model demand is calibrated to observations in the base year for regional totals but not at the decile level, so deciles reflect uncertainty in the base year. Then, with increasing income the parameters that create the highest near-term demand lead to the lowest levels of long-term demand (and vice-versa), producing a crossover point in demand where the uncertainty range shrinks to near zero.

https://doi.org/10.5194/egusphere-2026-3848
Preprint. Discussion started: 21 July 2026

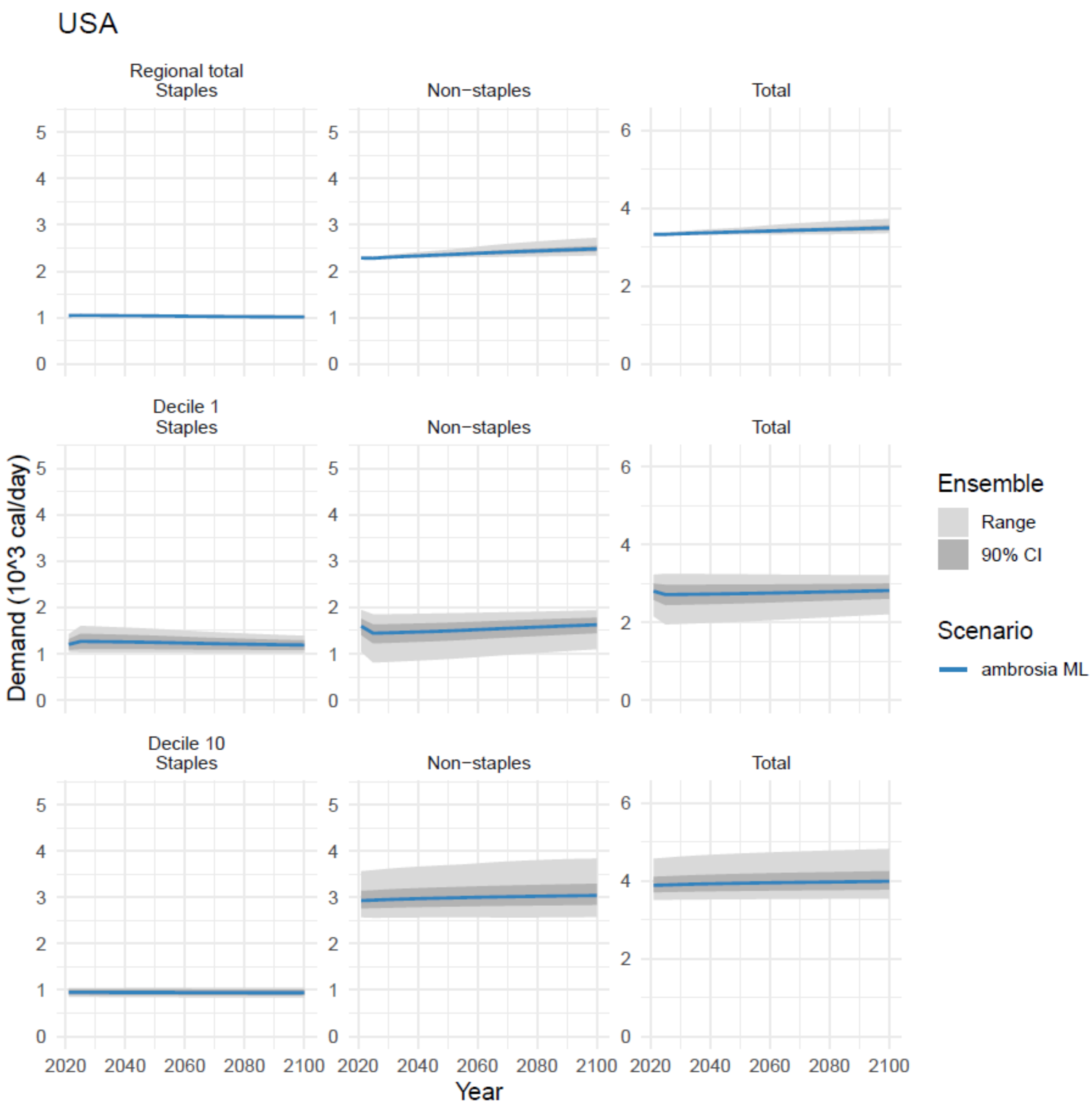

(a)

https://doi.org/10.5194/egusphere-2026-3848
Preprint. Discussion started: 21 July 2026

(b)

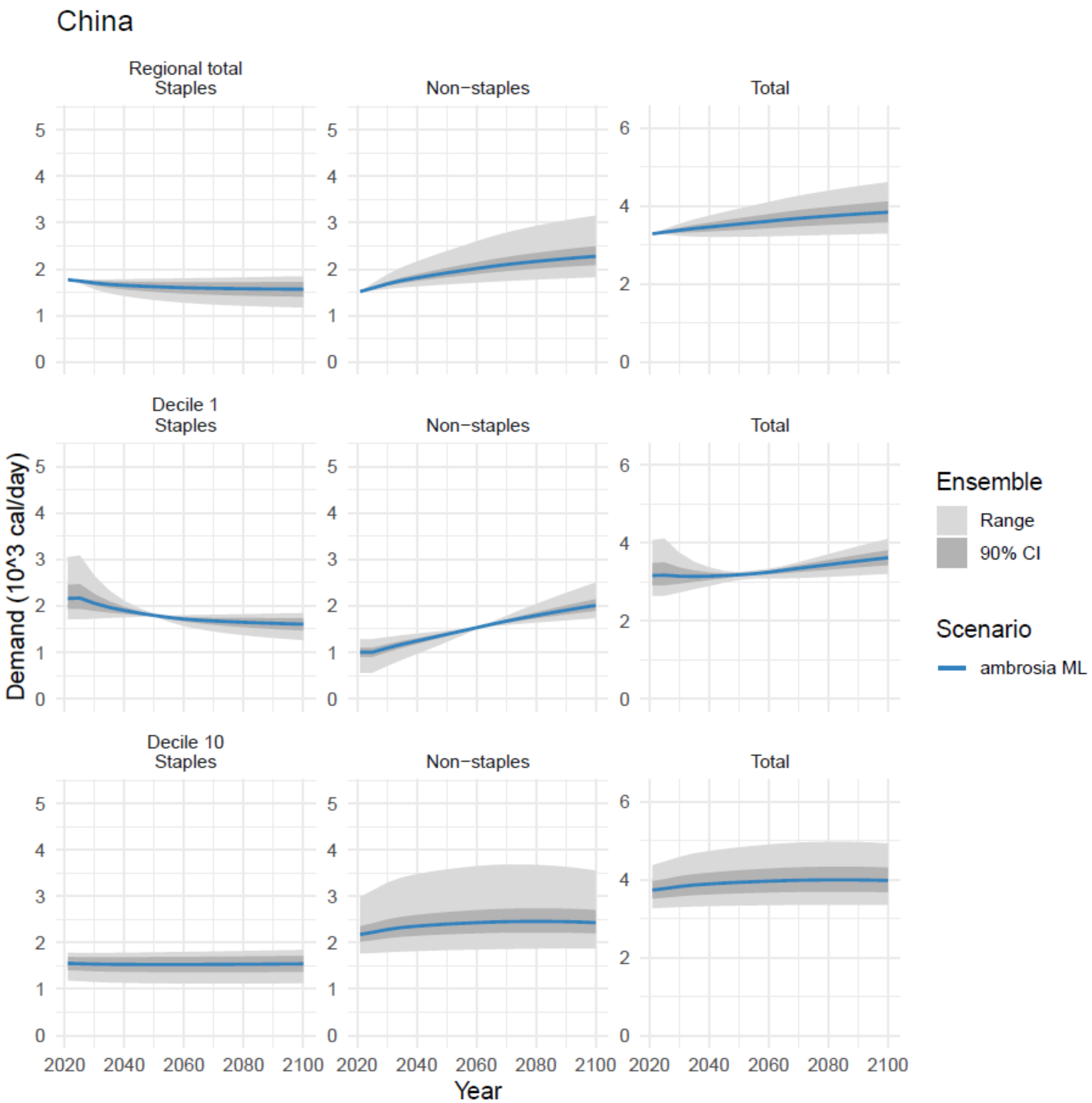

260 **Figure 5**: Food demand projected by ambrosia for (a) USA and (b) China for total regional demand (top row) and for demand from income deciles 1 and 10, as driven by per capita income and prices in the GCAM Reference scenario. Gray shaded regions indicate the range and 90% confidence interval of the ensemble of ambrosia simulations. Demand according to the maximum likelihood parameter values is in blue.

https://doi.org/10.5194/egusphere-2026-3848
Preprint. Discussion started: 21 July 2026

265 Figure 6 summarizes ranges of uncertainty in total demand across regions (see Fig. B5 for summaries of staples and non-staples demand). Regions with the largest uncertainty, prominently including South Asian and African regions as well as Central America & the Caribbean, have 90% confidence intervals in demand of ~300-500 cal/person/day in 2050 and ~600-800 cal/person/day in 2100. In contrast, higher income regions such as the US, Canada, Japan, and the EU have uncertainty of a few tens of cal/person/day in 2050, rising to up to ~200 cal/person/day in 2100.

(a)

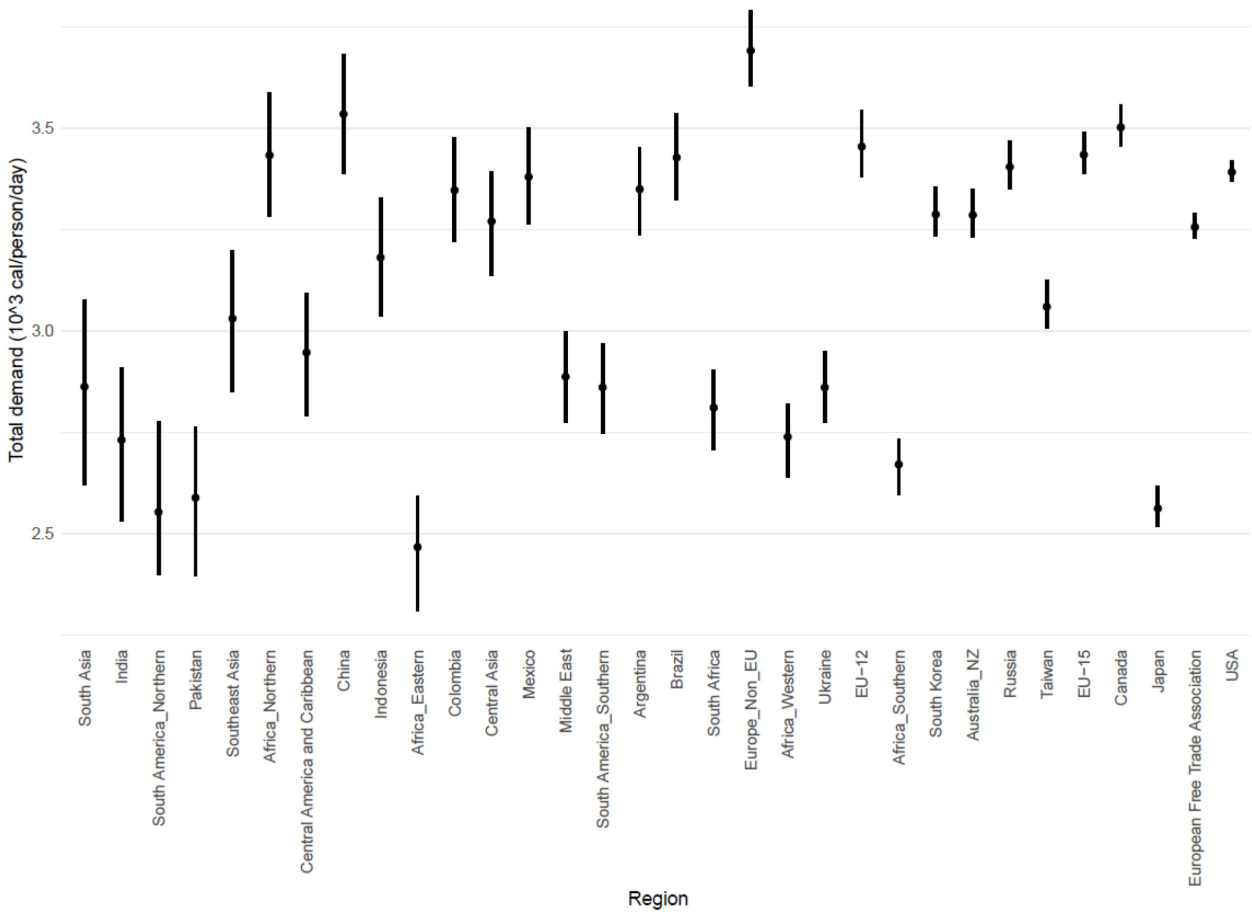

(b)

https://doi.org/10.5194/egusphere-2026-3848
Preprint. Discussion started: 21 July 2026

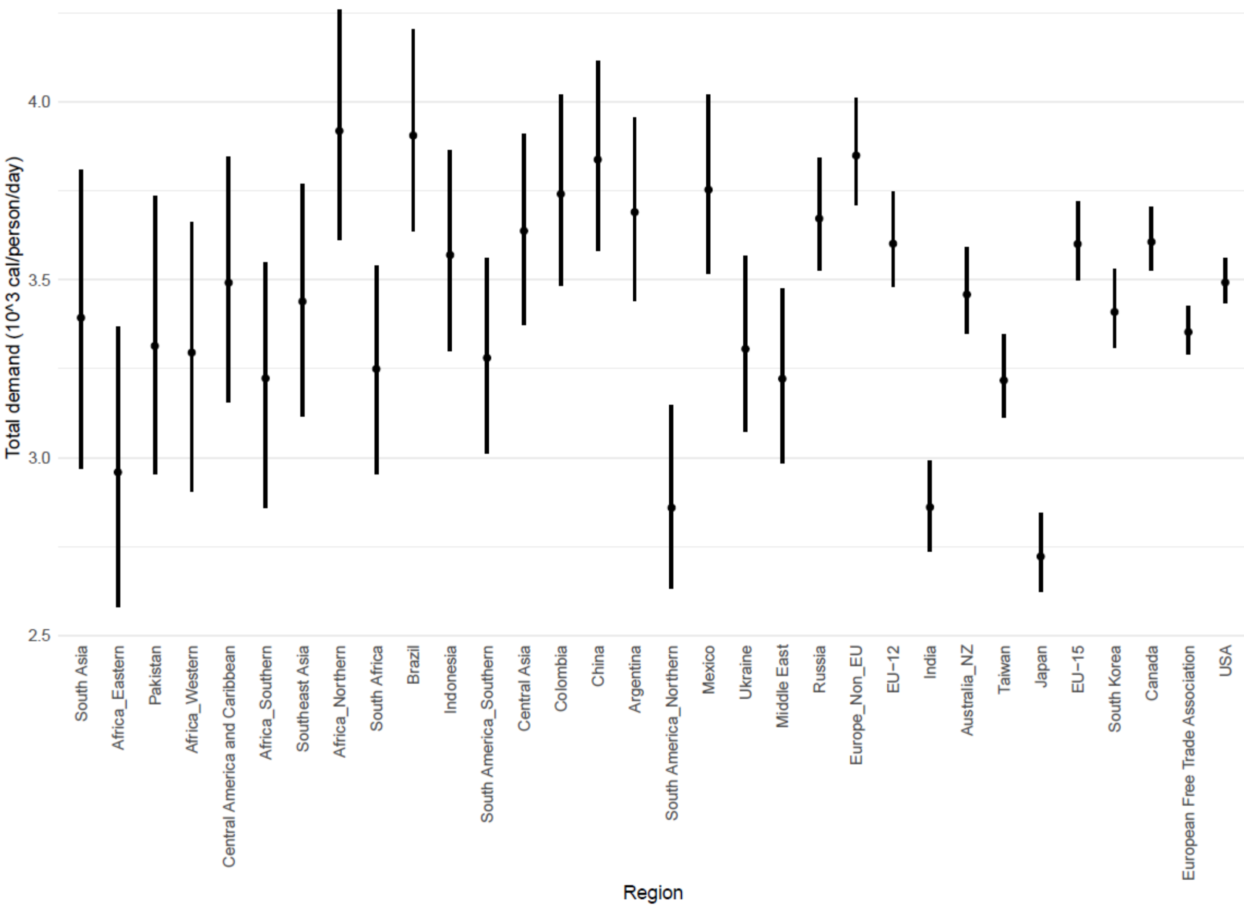

275

Figure 6: Uncertainty in total food demand in (a) 2050 and (b) 2100 for all GCAM regions. Bars span the 90% confidence interval and are arranged from largest to smallest (l-r). Figure B5 provides the same results for staples and non-staples.

https://doi.org/10.5194/egusphere-2026-3848
Preprint. Discussion started: 21 July 2026

This uncertainty is primarily driven by parameters that affect the response of demand to income. Varying these parameters alone while holding all others fixed at their maximum likelihood values produces a range of projected demand that is nearly as large as the total uncertainty due to all parameters (Fig. 7). Parametric uncertainty related to scale and response to prices also produce uncertainty in demand, but income parameters are sufficient to represent total uncertainty.

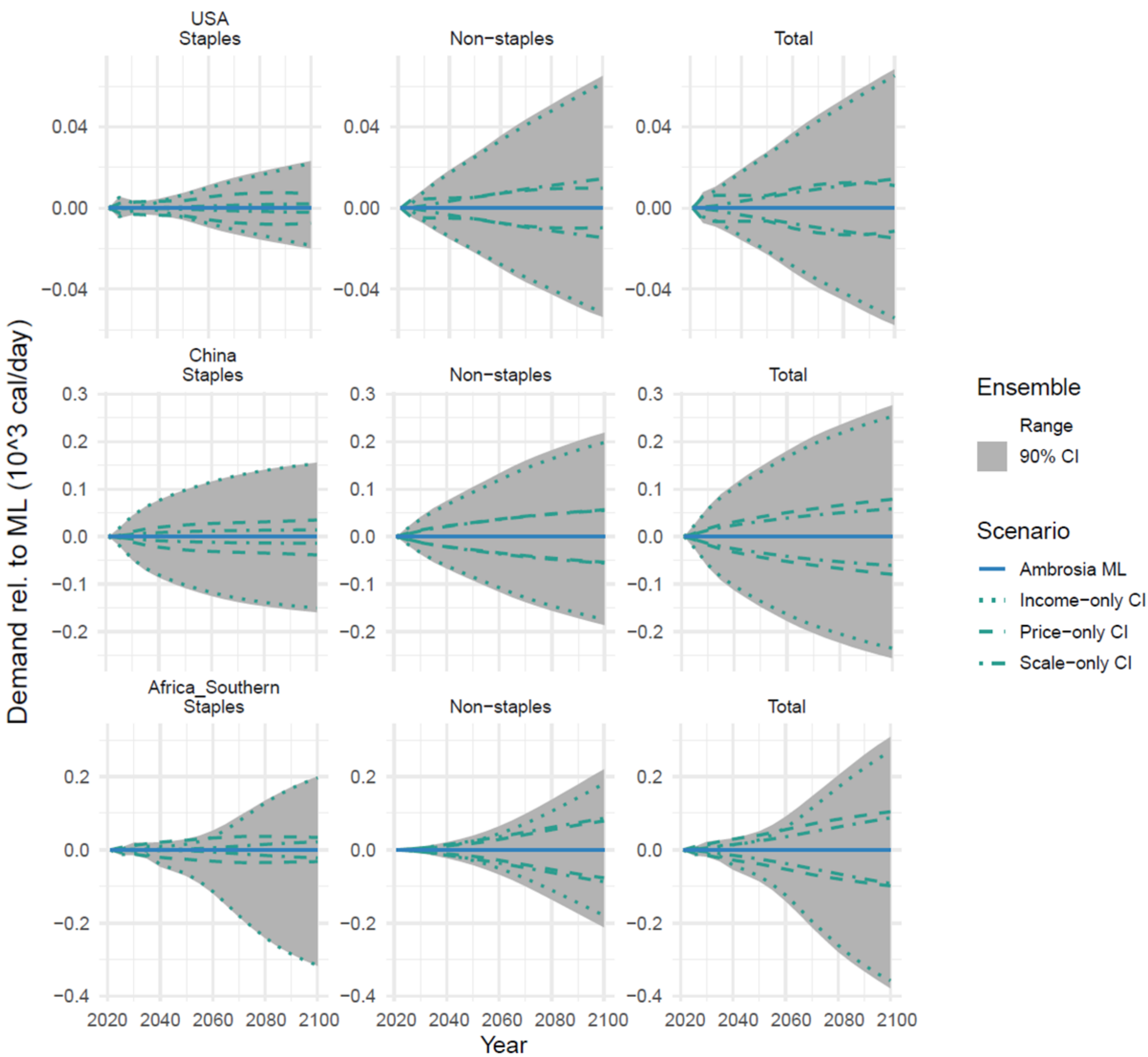

Figure 7: Decomposition of uncertainty in food demand into the separate effects of uncertainty in income (lambda, ks, eps1n), price (xi.ss, xi.nn, xi.cross), and scale (An, As, Pm, fixed effects) parameters for three selected regions.

https://doi.org/10.5194/egusphere-2026-3848
Preprint. Discussion started: 21 July 2026

3.2. Emulated uncertainty in the demand response to price changes

The ensemble of differences between emulated demand driven by high price conditions and by prices and income in the reference scenario shows that uncertainty in the demand response to price changes is also substantial, but varies much less across regions, deciles, and food type than does absolute demand (Figs. 8 and 9). As shown for the examples of the US and China, the 90% confidence interval of the change in demand is almost entirely negative, consistent with the intuitive expectation of the response to higher prices. It is generally larger for non-staples, except in low-income deciles which have a larger absolute demand for staples. Across regions, this confidence interval has a magnitude of ~150-200 cal/person/day in 2050, increasing to ~300-450 cal/person/day in 2100.

The extremes of the distribution of response to price changes are skewed toward positive values (Fig. 8). That is, while demand changes are predominantly negative, there is a small chance of substantial increases in demand due to increased prices. This can occur due to substitution effects (shifting, for example, from non-staples to staples as prices increase). There is also a long positive tail in changes in total food demand, but this is almost entirely made up of increases in one food type outweighing decreases in the other food type. In a very small number of cases, demand for both staples and non-staples increases simultaneously. Cross-price elasticities between the two goods are sufficiently large and symmetric in these cases that cross-substitution effects dominate own-price effects for both goods. This behavior likely reflects the flexibility of the demand system, which imposes some theoretical structure but still permits parameter combinations that generate economically unusual joint price responses.

https://doi.org/10.5194/egusphere-2026-3848
Preprint. Discussion started: 21 July 2026

(a)

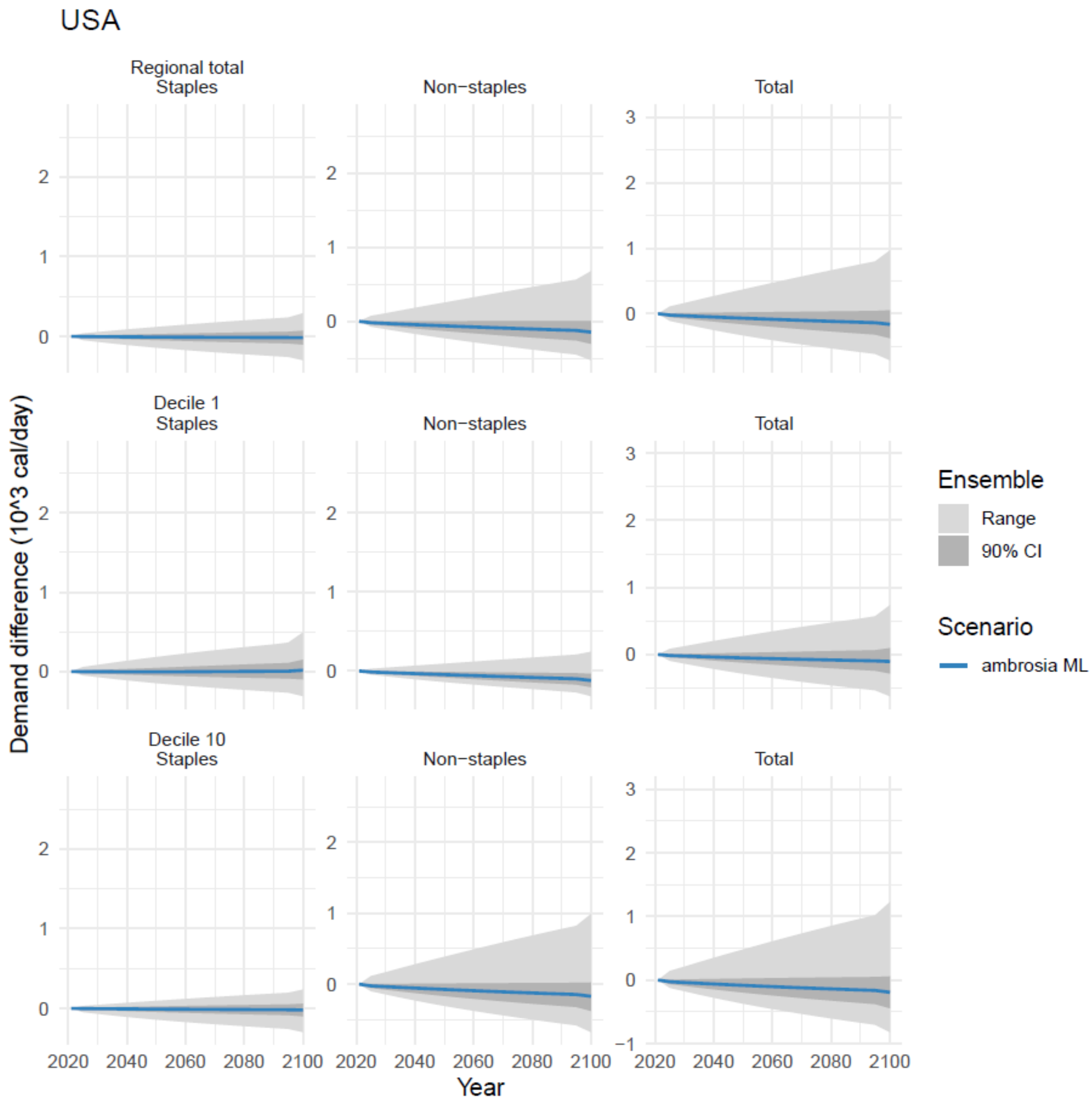

310

https://doi.org/10.5194/egusphere-2026-3848
Preprint. Discussion started: 21 July 2026

(b)

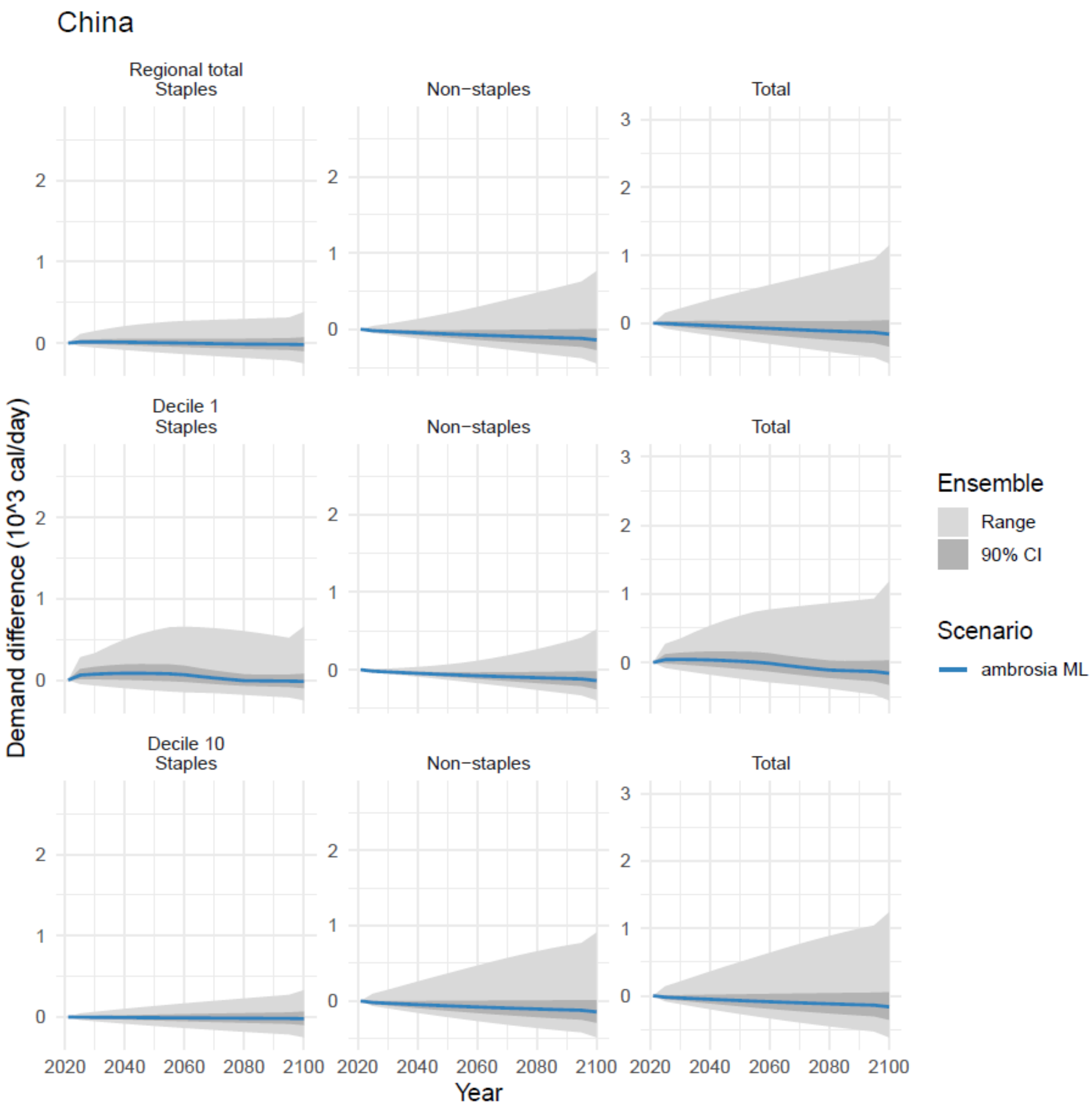

315 **Figure 8**: Differences in food demand due to price changes projected by ambrosia for (a) USA and (b) China for total regional demand (top row) and for demand from income deciles 1 and 10. Differences are calculated as demand with prices from the High Price Conditions scenario minus demand in the Reference scenario. Explanation of legend is as in Fig. 5.

https://doi.org/10.5194/egusphere-2026-3848
Preprint. Discussion started: 21 July 2026

(a)

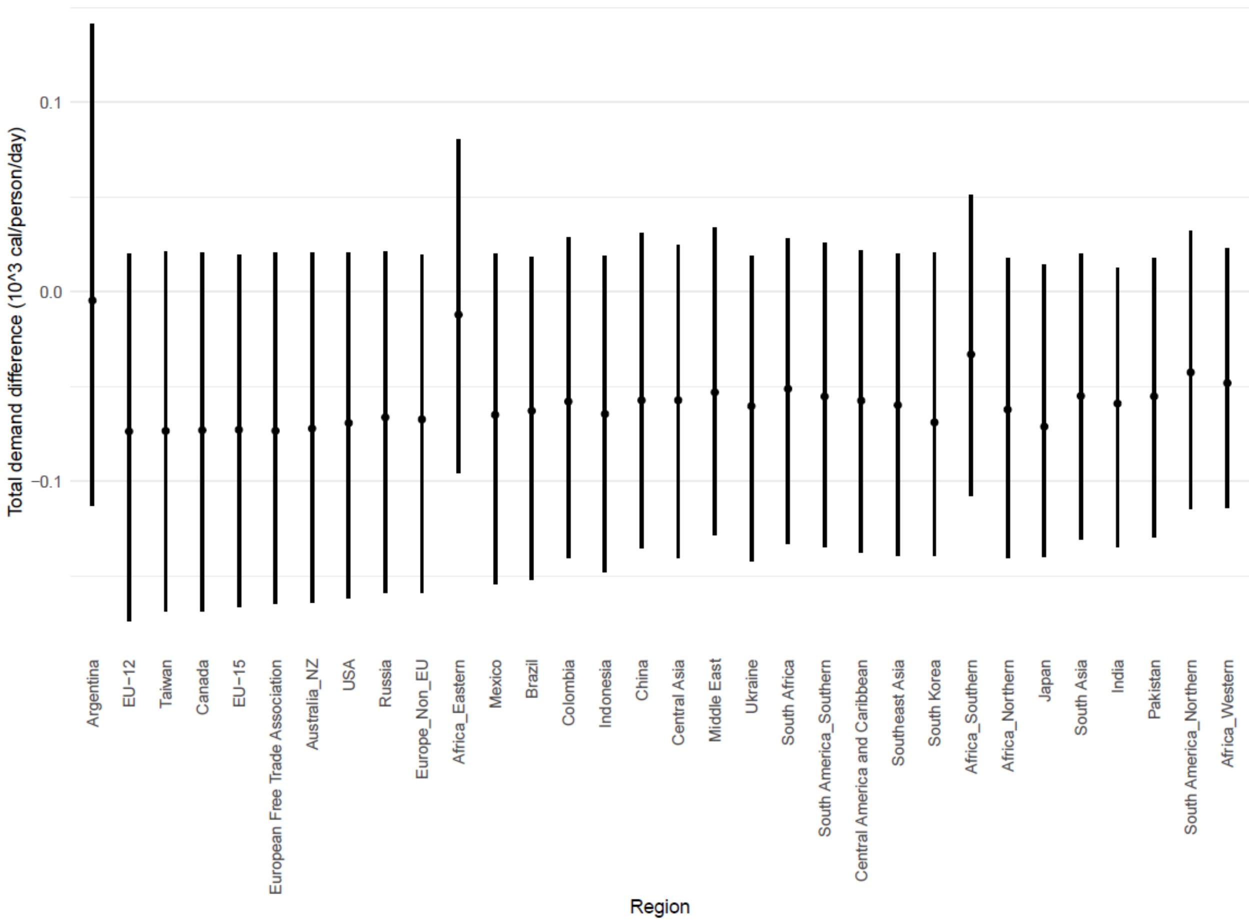

(b)

https://doi.org/10.5194/egusphere-2026-3848
Preprint. Discussion started: 21 July 2026

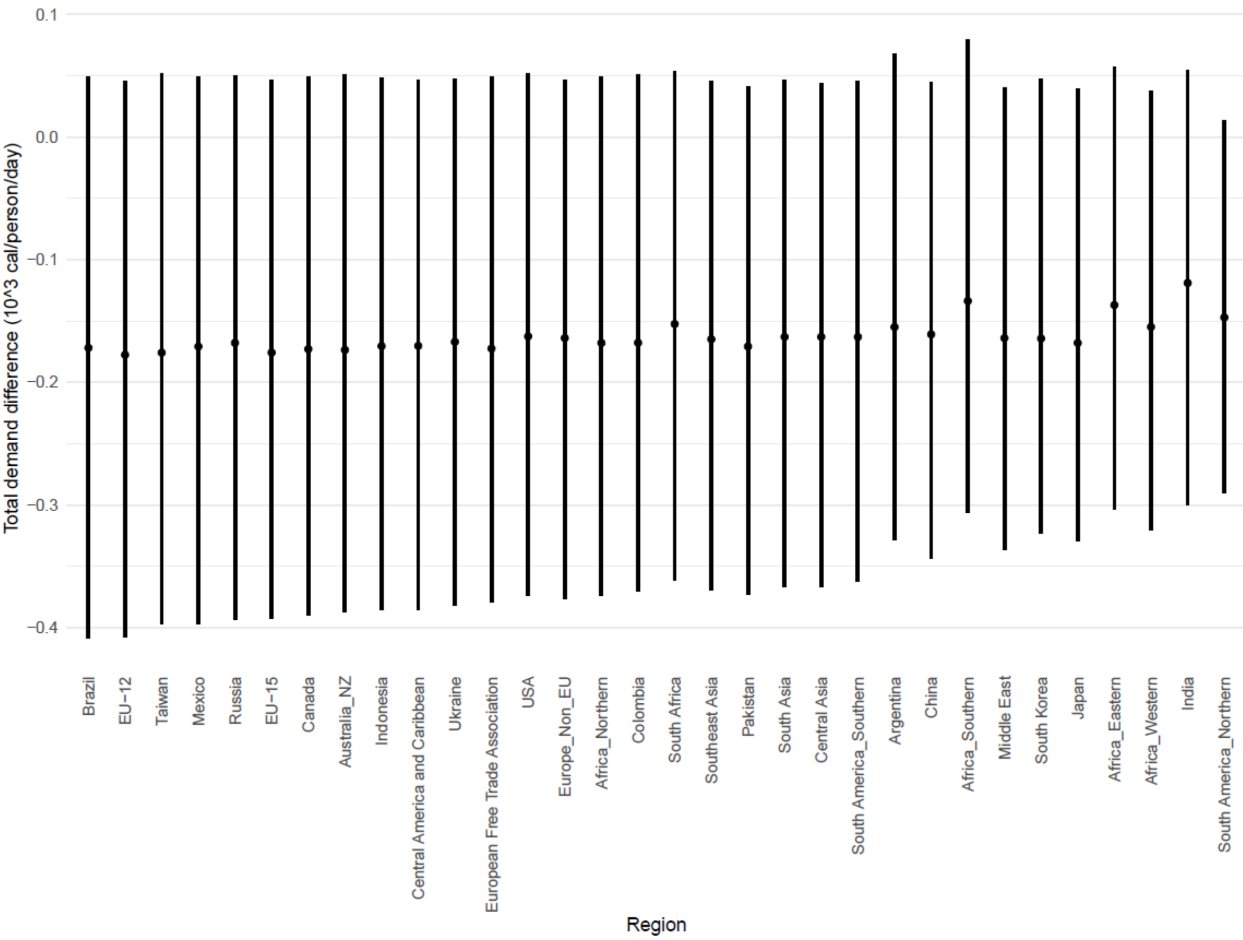

Figure 9: Uncertainty in differences in total food demand due to price changes in (a) 2050 and (b) 2100 for all GCAM regions. Bars span the 90% confidence interval and are arranged from largest to smallest (l-r). Figure B6 provides the same results for staples and non-staples.

The uncertainty in the response to price changes is driven almost entirely by the price-related parameters. Allowing these parameters to vary while holding all others fixed at their maximum likelihood values produces a range of projected demand that is the same size as the total uncertainty in demand (Fig. 10). Other parameters induce little uncertainty in the demand response.

The fact that income- and price-related parameters act largely independently on absolute demand and the price response suggests that a single set of parameters can be identified that has any desired combination of characteristics. One parameter set could produce, for example, both a relatively high absolute demand and a relatively low response to price changes (or a relatively high price response). The same applies to parameter sets producing relatively low absolute demand. This allows for the identification of four parameter sets that span both types of uncertainty simultaneously, which is pursued in the next section.

340

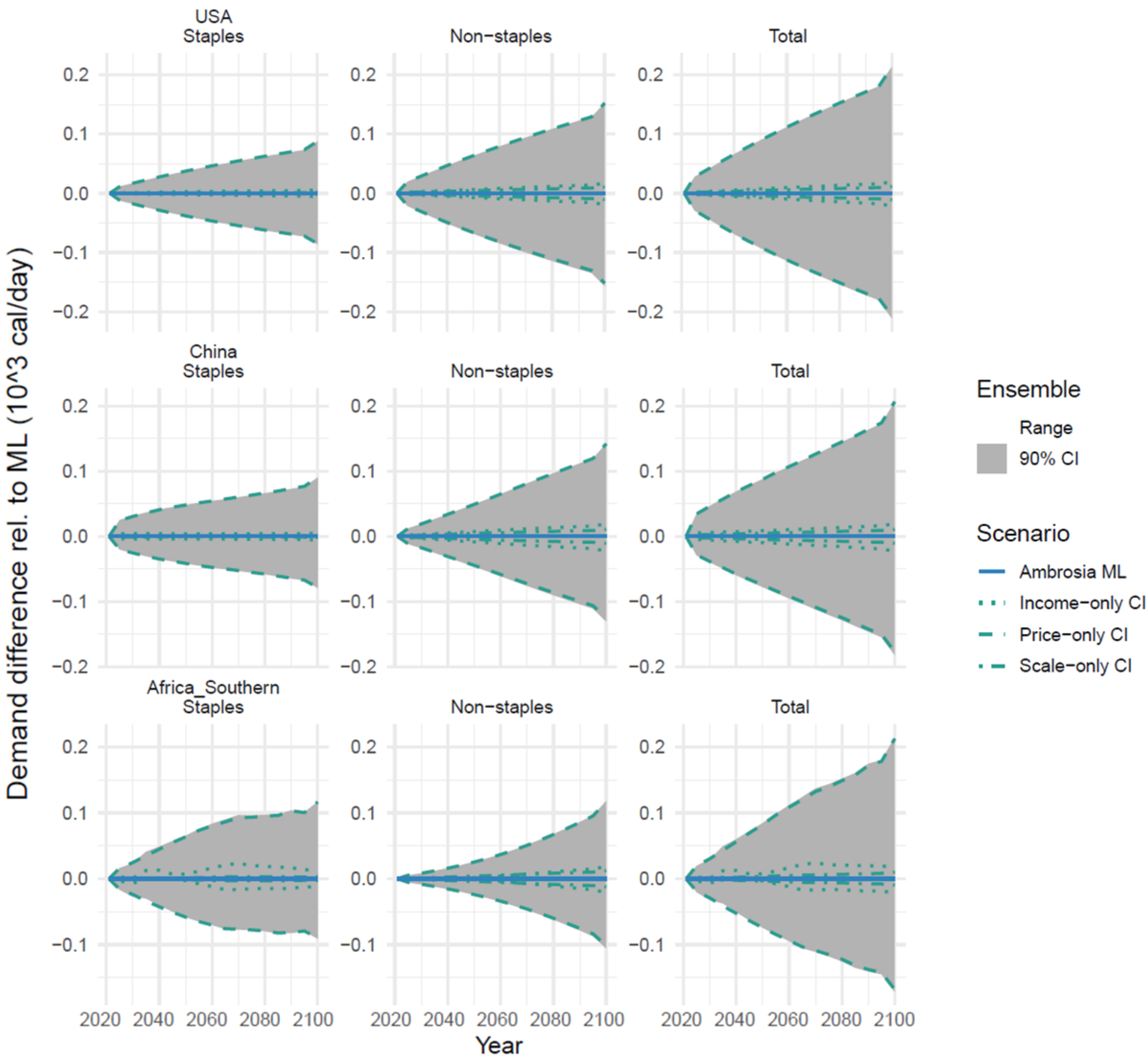

Figure 10: Decomposition of uncertainty in food demand response to price changes into the separate effects of uncertainty in income, price, and scale parameters for three selected regions.

3.3. GCAM scenarios representing demand uncertainty

https://doi.org/10.5194/egusphere-2026-3848
Preprint. Discussion started: 21 July 2026

As described in the methods section, parameter sets were identified that span the 90% confidence intervals of both total food demand and the change in total food demand in response to higher prices (as emulated with ambrosia) for the largest number of regions and time periods.

Figure 11 illustrates for a few example regions how GCAM scenarios that employ these parameter sets span the 90% confidence interval in emulated demand over time and regions, generally for both staples and non-staples (even though they were selected based on total food demand). As expected, whether the parameter sets reflect high or low response to price changes does not have much of an effect on absolute demand; the demand outcome is dominated by whether they are high or low demand parameter sets.

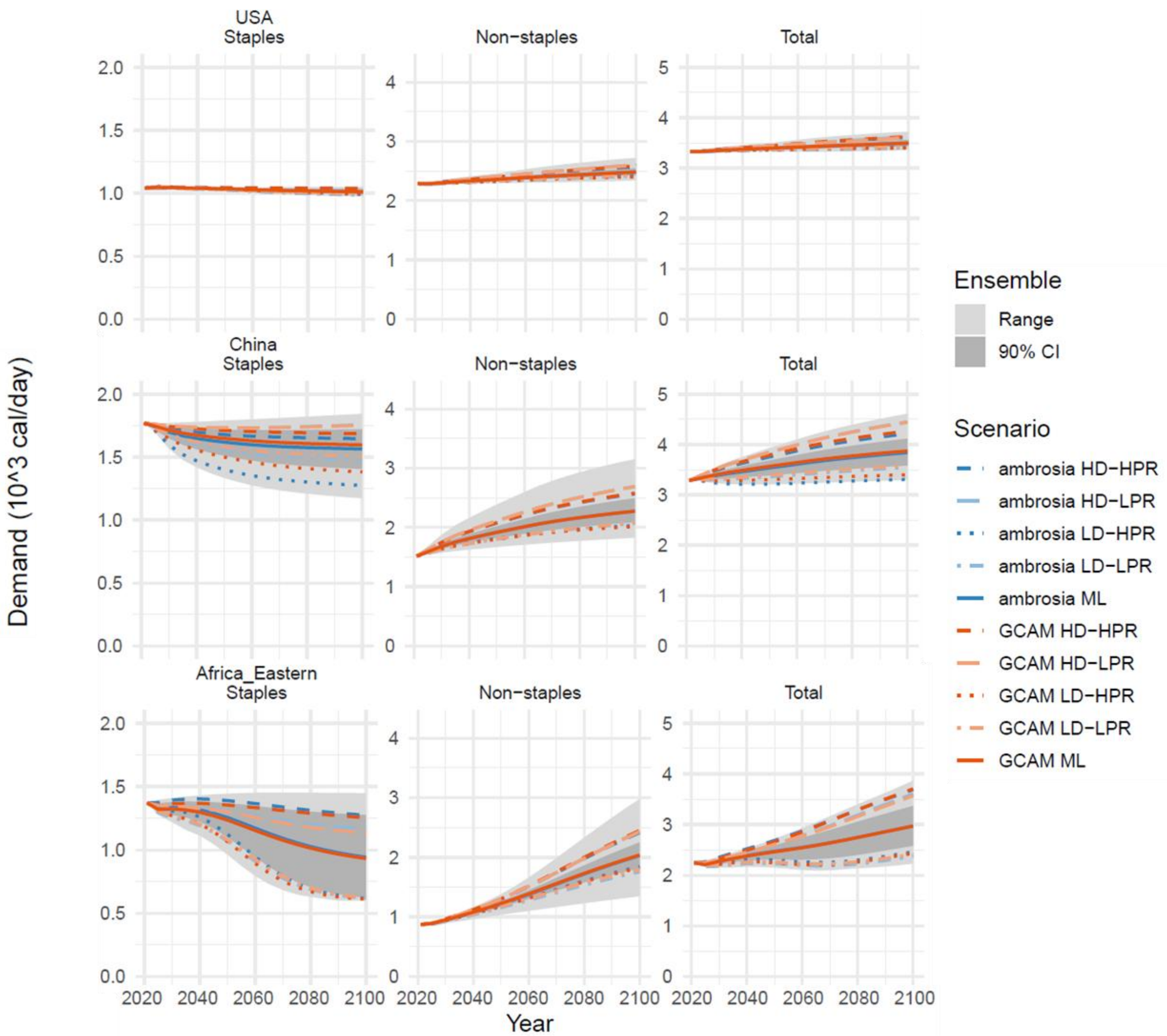

https://doi.org/10.5194/egusphere-2026-3848
Preprint. Discussion started: 21 July 2026

Figure 11: Projected food demand for USA, China, and Eastern Africa as driven by per capita income in the GCAM Reference scenario. Gray shaded regions indicate the range and 90% confidence interval of the ensemble of ambrosia simulations using prices from the GCAM Reference scenario. Orange lines indicate specific GCAM scenarios using maximum likelihood as well as High and Low Demand (each combined with High and Low Price Response) parameter sets. Blue lines indicate ambrosia scenarios based on the same sets of parameters. (Orange lines obscure blue lines in most cases.) Table C4 provides parameter values for each of the four scenarios.

Figure 11 also reflects the ability of ambrosia to emulate GCAM demand when parameters differ from their ML values. It illustrates the general finding that GCAM and ambrosia outcomes for the five parameter sets are very similar. China illustrates an exception for staples demand in the LD-HPR parameter set, where GCAM results are somewhat higher than ambrosia's. This kind of exception is rare: over 95% of ambrosia staples results, and 98% of non-staples results, across all regions, deciles, time steps, and parameter sets are within 5% of GCAM outcomes (see Fig. B6).

A summary of model comparison metrics for regional demand, demand across all deciles, and demand for decile 1 (the outcome most likely to differ) reinforces this view (Table C5). Correlations are high in all cases, typically ≥0.98 for aggregate outcomes and rarely falling below ~0.90, indicating that ambrosia reproduces well the structure of GCAM demand. Absolute errors are small, with RMSE typically in the range of ~0.007–0.045 for the ML and high demand cases and increasing under low demand scenarios, particularly for decile-level outcomes. The worst case occurs for staples demand in the LD–HPR scenario at the decile level (decile 1), where RMSE reaches 0.211 and MAE 0.080. This corresponds to an inaccuracy of roughly 80 cal/person/day on average (with larger deviations captured by RMSE of about 200 cal/person/day), which remains modest relative to typical total consumption levels of 2,000–3,000 cal/person/day. Errors are consistently largest at the decile level and smallest for regional aggregates and are generally larger for staples and total demand than for non-staples. Biases are small overall, with mild underprediction in low demand cases and slight overprediction in high demand cases.

Exceptions to this overall performance include staples demand in low income deciles in Argentina, South America Northern (dominated by Venezuela), and to a lesser extent Africa Eastern and China (as already noted). Particularly in the two South American regions, differences reflect GCAM solver difficulties given very large declines and then reversals in income between 2015 and the 2021 base year.

Ambrosia is similarly effective in emulating GCAM's response to increases in food prices. Figure 12 illustrates the results for the same three regions as in Fig. 11: the US and China show very similar demand changes across models for all parameter sets. Eastern Africa illustrates an exception, where the ML and High Price Response scenarios show clear

https://doi.org/10.5194/egusphere-2026-3848
Preprint. Discussion started: 21 July 2026

differences. Again, this kind of exception is rare: over 95% of ambrosia staples and non-staples results across all regions, deciles, time steps, and parameter sets are within 50 calories/person/day of GCAM outcomes (Fig. B7).

A summary of model comparison metrics for changes in demand in response to price changes (Table C6) indicates that ambrosia emulation of GCAM is generally good, though less precise than the case of absolute demand in the Reference scenario. Correlations remain high for aggregate outcomes, typically above 0.9 for total demand and non-staples. Performance is more uneven at the decile level, particularly for staples and for non-staples in high price response cases, where correlations can fall substantially and, in a few cases, become negative. Absolute errors are correspondingly larger and more variable, particularly for staples demand in the LD–HPR scenario and for non-staples demand in the HD–HPR scenario at the decile level, where RMSE reaches approximately 0.17 and 0.11, respectively, with MAE on the order of 0.04–0.08. These correspond to 40–80 cal/person/day on average (with larger deviations reflected in RMSE values above 100 cal/person/day).

https://doi.org/10.5194/egusphere-2026-3848
Preprint. Discussion started: 21 July 2026

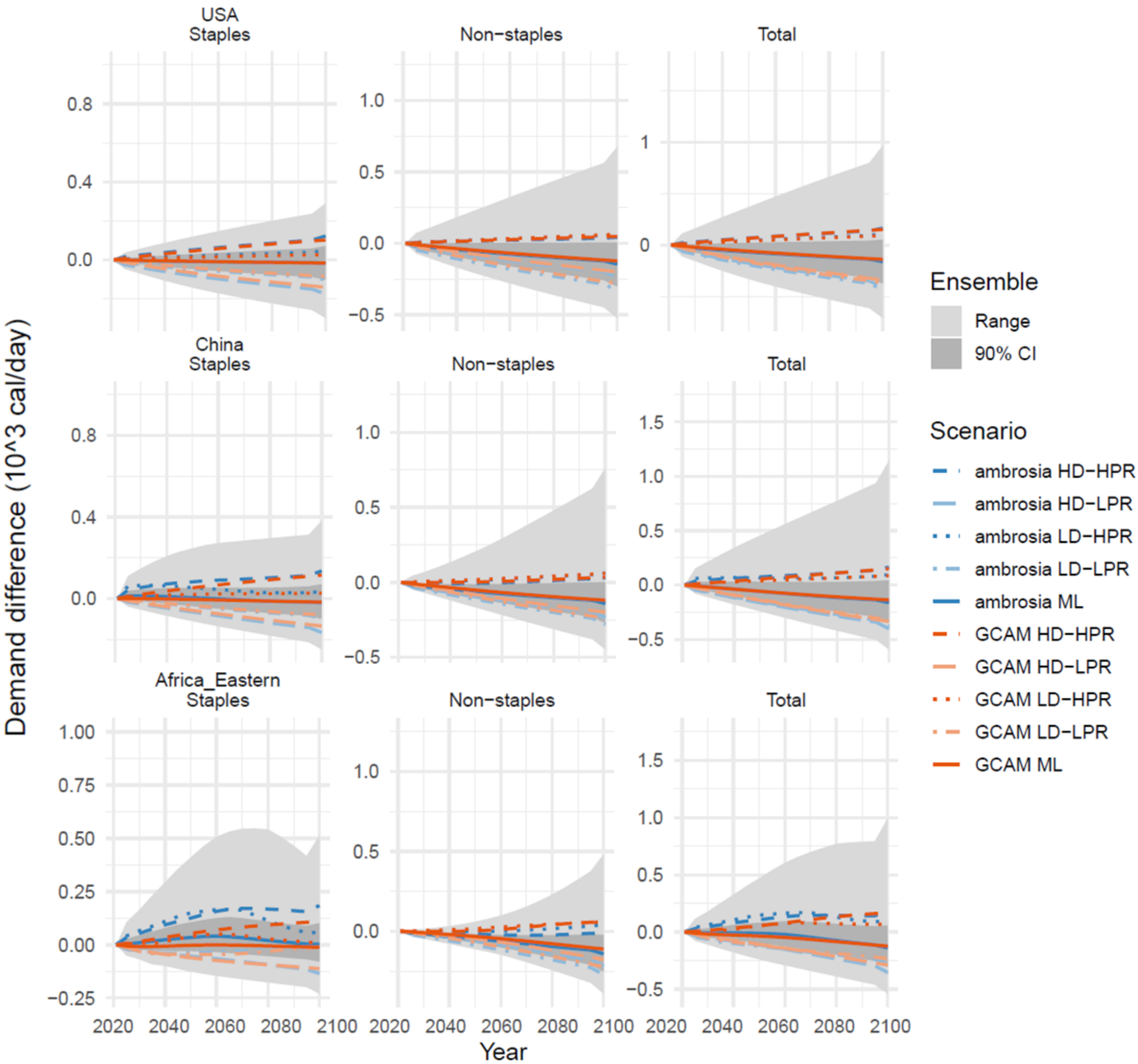

Figure 12: Same as Fig. 11 but for differences in demand.

3.4. Implications for other sectors

Given the cross-sectoral linkages between food consumption and land, water, and energy use, we examined the uncertainty in these outcomes that can be driven by uncertainty in food demand. The GCAM scenarios based on the five parameter sets show that in particular regions, outcomes can be sensitive to variations in food demand (Fig. 13). For example, in the US, land used for crop growth varies by more than 100,000 km2 by the end of the century due to the uncertainty in food demand, a substantial fraction of the 500,000 km2 used in the ML case. Similarly, in Brazil, pasture used for grazing livestock varies

https://doi.org/10.5194/egusphere-2026-3848
Preprint. Discussion started: 21 July 2026

by about 250,000 km2 by 2100, about 10% relative to the ML case. Pasture shows a similar uncertainty range in Eastern Africa, where biomass production for energy use also varies across a range representing about 50% of the production in the ML case. These regional patterns are determined by food demand uncertainty in the same regions but also by trade patterns that can link uncertainty in food demand in one region to production in another.

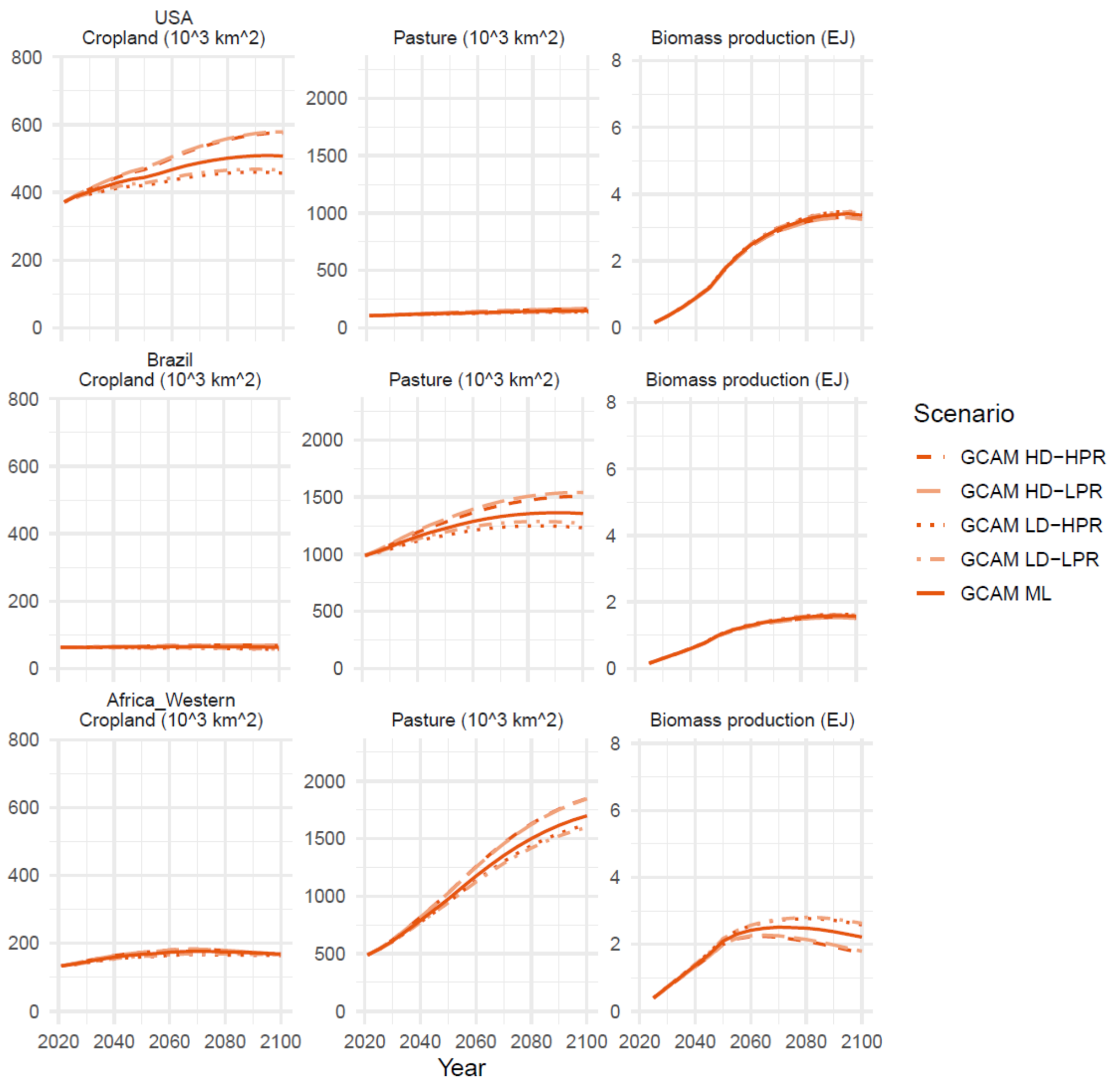

Figure 13: Projected land use for crops, water withdrawals, and biomass production in the USA, India, and Western Africa in the GCAM Reference scenario with the five parameter sets.

https://doi.org/10.5194/egusphere-2026-3848
Preprint. Discussion started: 21 July 2026

4. Conclusions

In this study we quantified the uncertainty in projected food demand across world regions due to uncertainty in the parameters of the food demand system in the Global Change Analysis Model (GCAM). We also introduced heterogeneity in food demand within regions, across income deciles of the population, and examined parametric uncertainty at this level. Our approach was based on the generation of ensembles of thousands of simulations with an emulator of food demand in GCAM. Running large ensembles with a multisector dynamics model like GCAM is not feasible in many applications, so we proposed a means of accounting for this uncertainty in a small number of alternative scenarios that captures not only uncertainty in demand but also in the response of demand to price changes. Finally, we demonstrated how parametric uncertainty in food demand can propagate to other sectors.

We found that parametric uncertainty varied across regions and deciles but could be substantial relative to other sources of uncertainty. It is particularly large in regions in South Asia, Africa, and Central America and the Caribbean and in low-income deciles, conditions which are less well-constrained by historical data. Methodologically, we demonstrated that a scenario discovery-type approach can be a useful way to identify parameter sets that represent multiple dimensions of uncertainty simultaneously.

Limitations of this work include data availability for parameter estimation. We use national-level data, aggregated to 32 GCAM regions, to estimate parameters appropriate to the regional level at which they are employed. The lack of comparable data specific to sub-populations (such as income deciles) within regions means that parameters are not estimated separately across these groups and also that modeled values for these groups in the base year are not calibrated to observations. Such data are typically available only from household surveys for individual countries, and often these data do not include all necessary variables: quantities, expenditures, prices, and income. Collection and processing of such data is a laborious (and sometimes costly) undertaking (O'Neill et al., 2020), with limits to the coverage ultimately obtainable.

Future work could introduce parameter estimation at the decile level for a small number of countries where data are available to test the improvement that could be made over the use of national level data. In addition, we use per capita GDP as a measure of income when estimating parameters given that it is the measure used in the GCAM demand system. However, it would be more appropriate to model food demand with household disposable income. A new version of GCAM with an explicit representation of the government and household sectors is under development that would generate household income endogenously and could be used for this purpose.

Appendix A

Appendix A contains additional text.

A1. Food demand functions

The food demand functions are the same as those in Edmonds et al. (2017) with the exception of the addition of the regional fixed effects for staples and the minimum demand thresholds:

$$q_{s,r} = F_{s,r} + A_s\left(x_r^{h_s(x)}\right)\left(w_{s,r}^{e_{ss}(x)}\right)\left(w_{n,r}^{e_{sn}(x)}\right) \quad \text{(A1)}$$

$$q_{n,r} = A_n\left(x_r^{h_n(x)}\right)\left(w_{s,r}^{e_{ns}(x)}\right)\left(w_{n,r}^{e_{nn}(x)}\right) \quad \text{(A2)}$$

where $q_{s,r}$ and $q_{n,r}$ are per capita demand for staples and non-staples in region r, respectively; $F_{s,r}$ is a regional staples fixed effect; A_s and A_n are parameters; x is income; w is price; and h and e are income and price elasticities (own- and cross-), respectively. Minimum demand thresholds are $q_{s,r} \geq 600$ cal/person/day and $q_{n,r} \geq 0$ cal/person/day. The threshold for staples consumption is low enough to identify households with high food insecurity risks, the main outcome of interest under low-demand conditions.

Income elasticities are determined as:

$$h_s(x_r) = \left(\frac{\lambda}{x_r}\right)\left(1 + \frac{\kappa}{\ln(x_r)}\right) \quad \text{(A3)}$$

$$h_n(x_r) = \left(\frac{\nu}{1-x_r}\right) \quad \text{(A4)}$$

where λ, κ, and ν are parameters. Price elasticities are determined as:

$$e_{ij}(x_r) = g_{ij} - h_i(x_r)\alpha_j \quad \text{(A5)}$$

where i and j are food types (staples or non-staples), g_{ij} is a parameter (three total: g_{ss}, g_{nn}, $g_{sn} = g_{ns}$), and α_j is the budget share for food type j.

https://doi.org/10.5194/egusphere-2026-3848
Preprint. Discussion started: 21 July 2026

A2. Parameter estimation

For the MCMC parameter estimation, we use the constraints on parameter values shown in Table C1. These are meant to reflect physical constraints and economic expectations, as well as to ensure reasonable structure of the demand functions. The scale parameters (As, An) should be non-negative; the parameters for own-price elasticities non-positive; the parameters for income response non-negative (and for the location of the peak in staples demand, non-zero as well); and the materials price should be positive.

The likelihood function is

$$\ln(L) = \sum_{i=1}^{N} \frac{(y_i - \hat{y}_i)^2}{2\sigma_i^2} \qquad \text{(A6)}$$

where y_i and $\hat{y}_i$ are the i-th observed and predicted consumption value, respectively, and σ is the standard deviation in the observations for observation i.

This form implies that errors are independent and normally distributed. It requires estimates of the standard deviation of observational errors, which are not provided by FAO. We use the same approach as described in Edmonds et al. 2017: a Divisive Analysis (DIANA) clustering algorithm to cluster the observed economic data based on regional incomes and prices and calculate standard deviation values for each group. This approach treats the groups as proxies for repeated independent measurements of consumption.

The MCMC estimation was initiated with the maximum likelihood parameter values from Edmonds et al. (2017). The standard deviation of the proposal distribution was initially 0.05 and then tuned every 100 iterations during the burn-in period to approach a target proposal acceptance rate of 20%. The burn-in period was determined to be about 70,000 iterations before the posterior distribution became stable as determined by trace plots.

A3. Identification of alternative parameter sets

The process of identifying alternative parameter sets based on ambrosia ensembles started by identifying all parameter sets whose ambrosia total food demand pathways for a given region and time step lie above the 90% confidence interval in the Reference pathway. This produces 50 parameter sets, given that the full distribution contains 10 thousand. This step is repeated for each time step and region. We then do the same for parameter sets that lie below the 90% confidence interval. We then repeat both of these steps for the uncertainty distribution in the response of total food demand to price changes.

https://doi.org/10.5194/egusphere-2026-3848
Preprint. Discussion started: 21 July 2026

We use these results to identify parameter sets that span uncertainty for the largest number of regions and time steps. For reasons discussed further in the Results section, we look for parameters that simultaneously represent High Demand (HD) combined with either High or Low Price Response (HPR, LPR), as well as parameters that simultaneously represent Low Demand (LD) combined with either HPR or LPR. In each of these four cases, we search across 512 groups (32 regions x 16 time steps) of 50 parameter sets each. We identify parameter sets that appear in the largest number of these groups.

For example, in the HD-HPR case, we rank parameter sets by the number of times they appear in the 512 groups representing High Demand and High Price Response. Table C3 summarizes results, showing that the best parameter set falls simultaneously within the High Demand interval and the High Price Response interval 507 times (out of a possible 512). The best parameter set for the other cases fall within the 512 groups a minimum of 447 times (for LD-HPR).

Appendix B

Appendix B contains additional figures.

https://doi.org/10.5194/egusphere-2026-3848
Preprint. Discussion started: 21 July 2026

B1. Posterior parameter distributions

Figure B1: Posterior distributions of regional fixed effect parameters for the food demand function, with maximum likelihood (ML) values marked by the red vertical line.

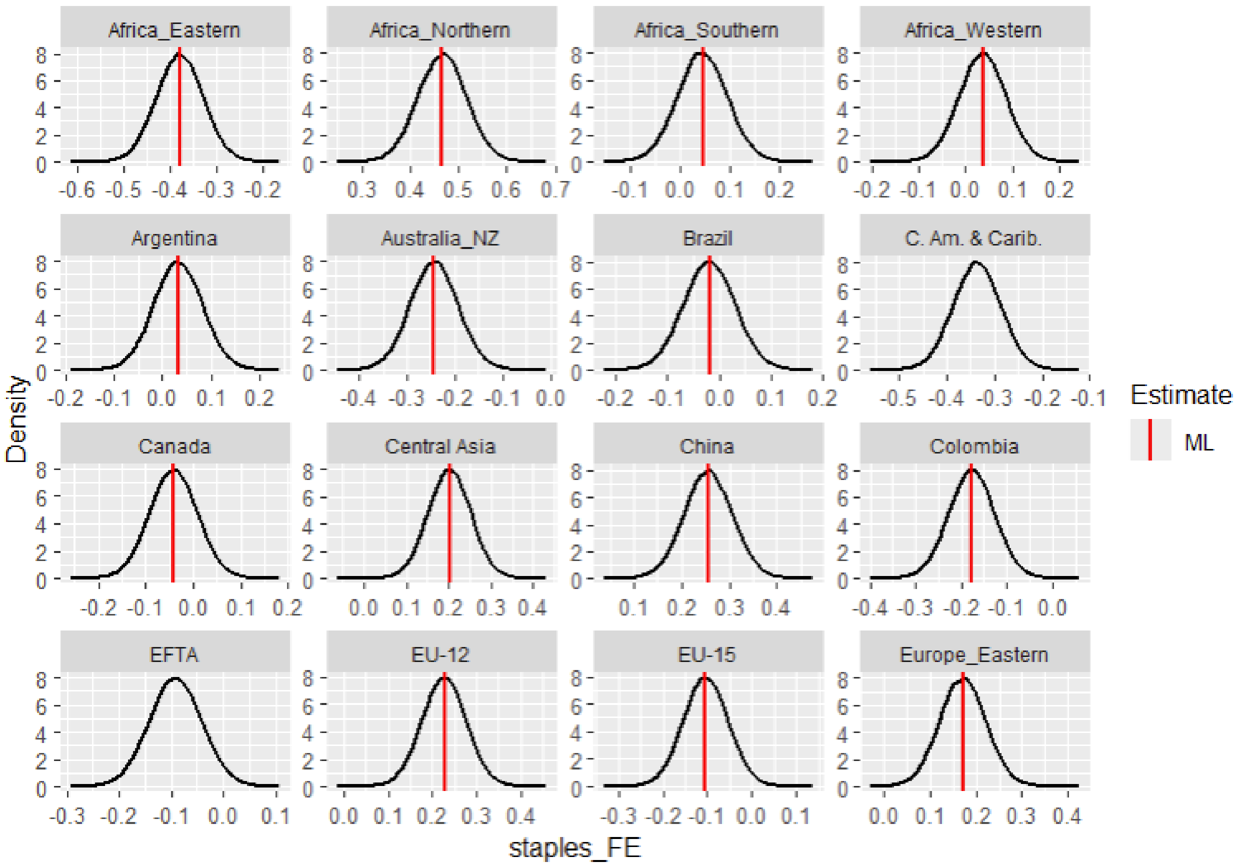

525

https://doi.org/10.5194/egusphere-2026-3848
Preprint. Discussion started: 21 July 2026

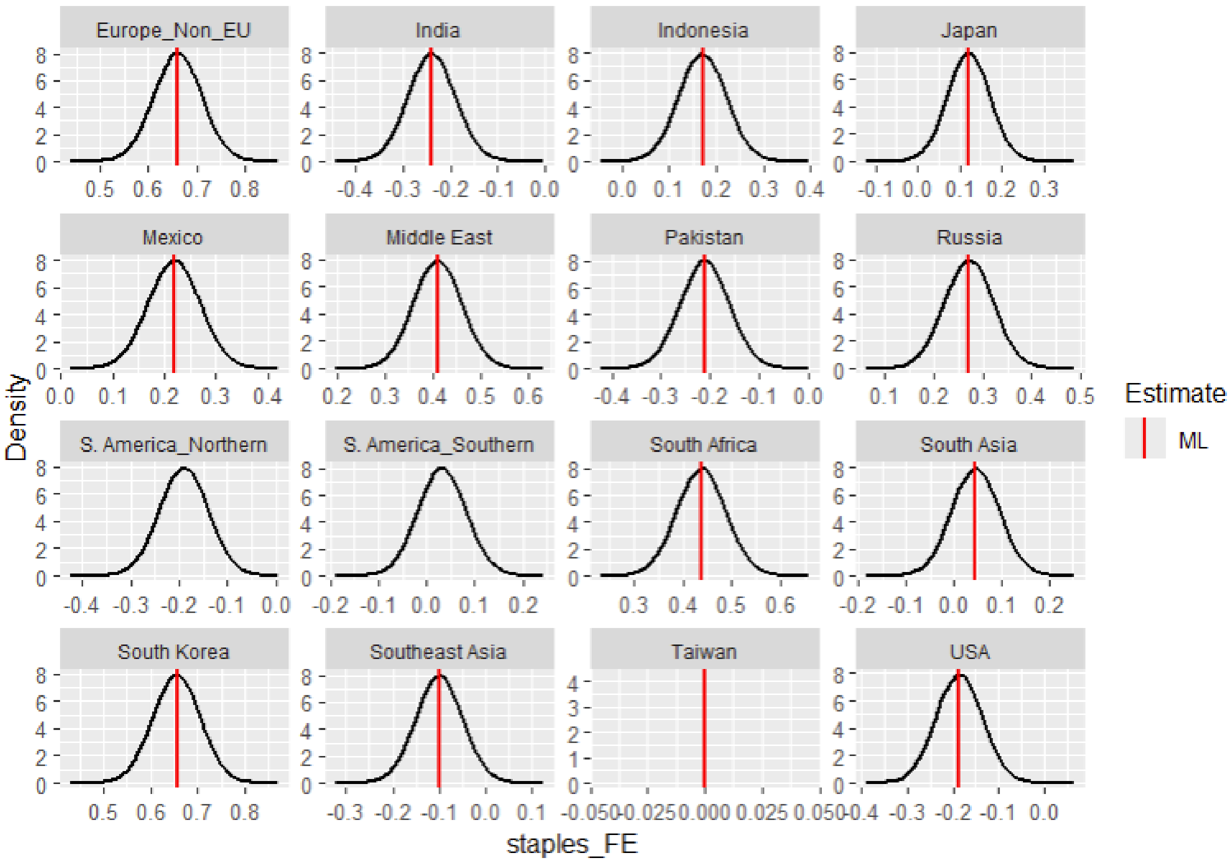

https://doi.org/10.5194/egusphere-2026-3848
Preprint. Discussion started: 21 July 2026

B2. Implied elasticities

Figure B2: Implied price and income elasticities of demand as a function of income for this study as compared to parameters derived for the GCAM model in studies in 2017 (Edmonds et al., 2017) and a 2021 update. Elasticities assume constant
530 prices at typical values (Ps = 0.05, Pn = 0.25). The x-axis is shown on a square-root scale to make results at low incomes clearer.

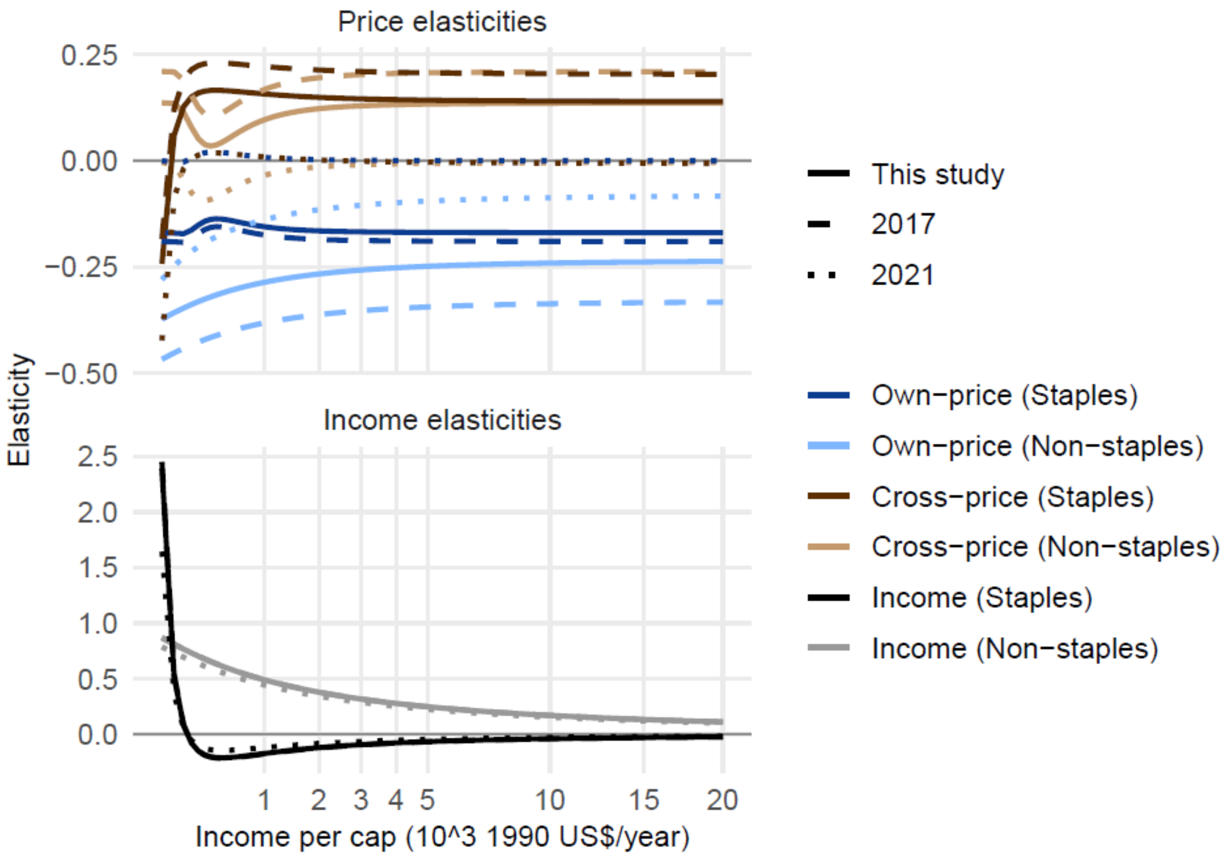

B3. Model fit to observations

Figure B3: Modeled (ambrosia) versus observed food demand for 1254 observations. Each row shows results for a specific
535 set of parameters.

https://doi.org/10.5194/egusphere-2026-3848
Preprint. Discussion started: 21 July 2026

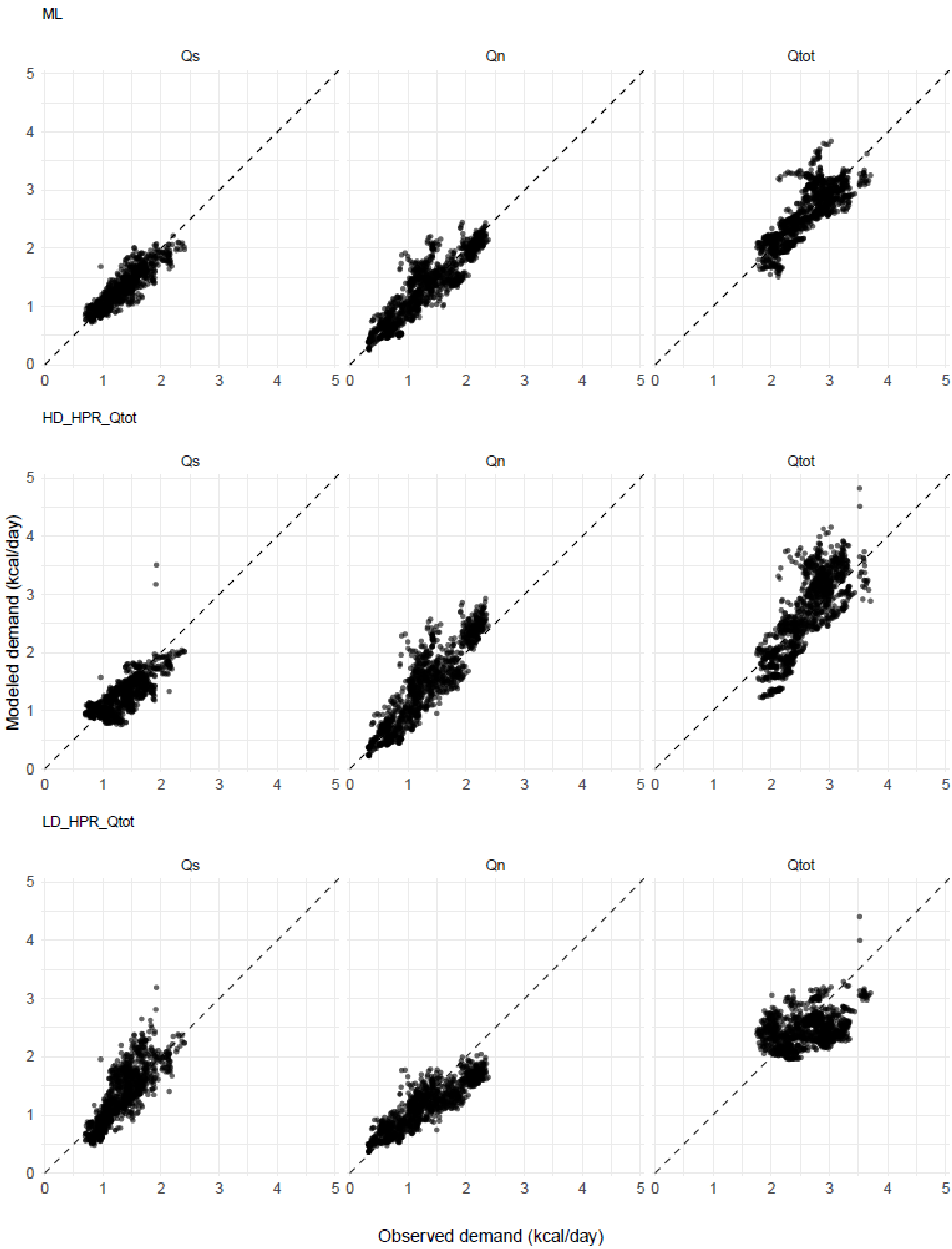

https://doi.org/10.5194/egusphere-2026-3848
Preprint. Discussion started: 21 July 2026

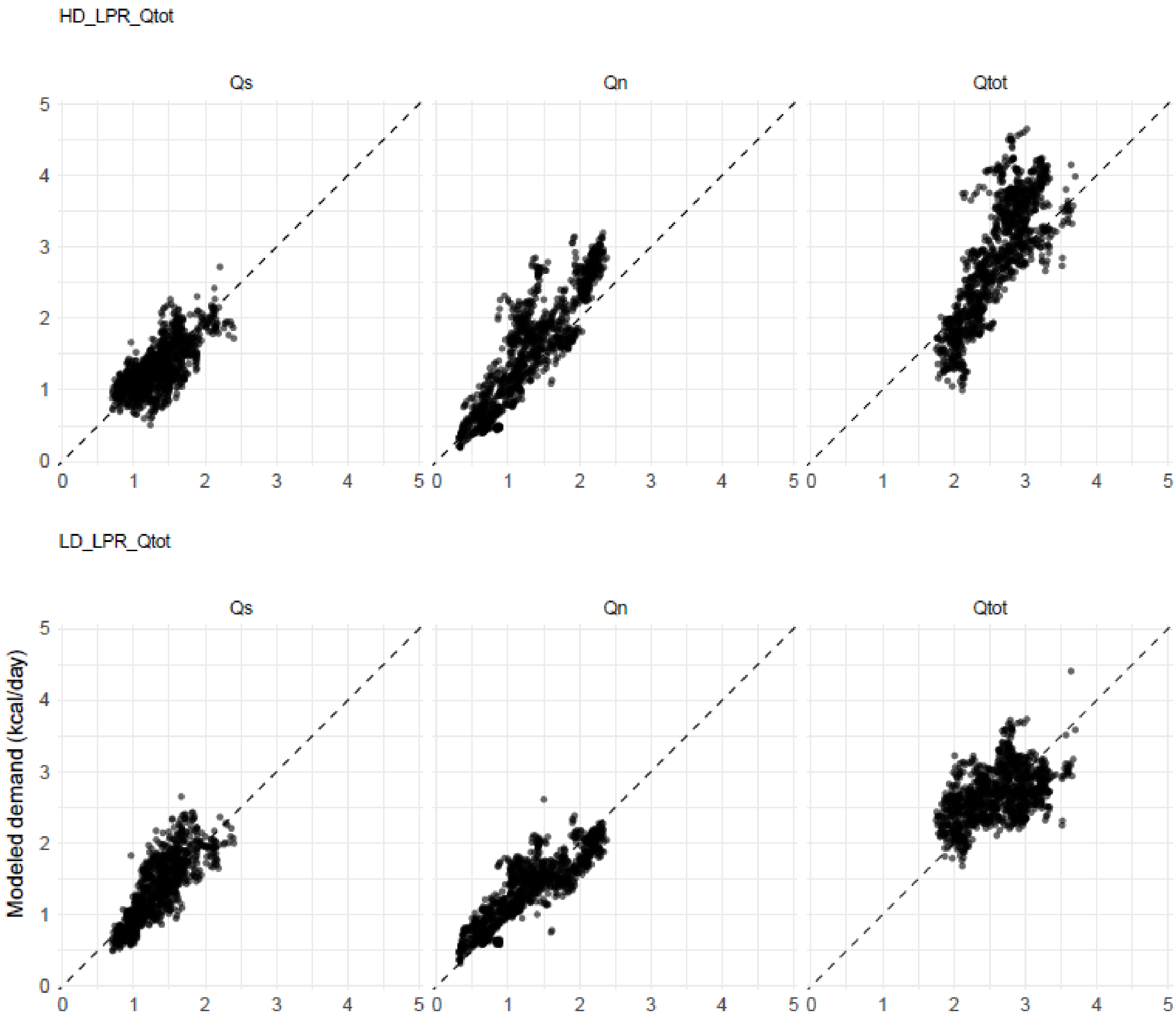

540 Figure B4: Modeled (ambrosia, in orange) versus observed (gray) food demand as a function of per capita income, for the same observations as in Figure B3. Each row shows results for a specific set of parameters.

https://doi.org/10.5194/egusphere-2026-3848
Preprint. Discussion started: 21 July 2026

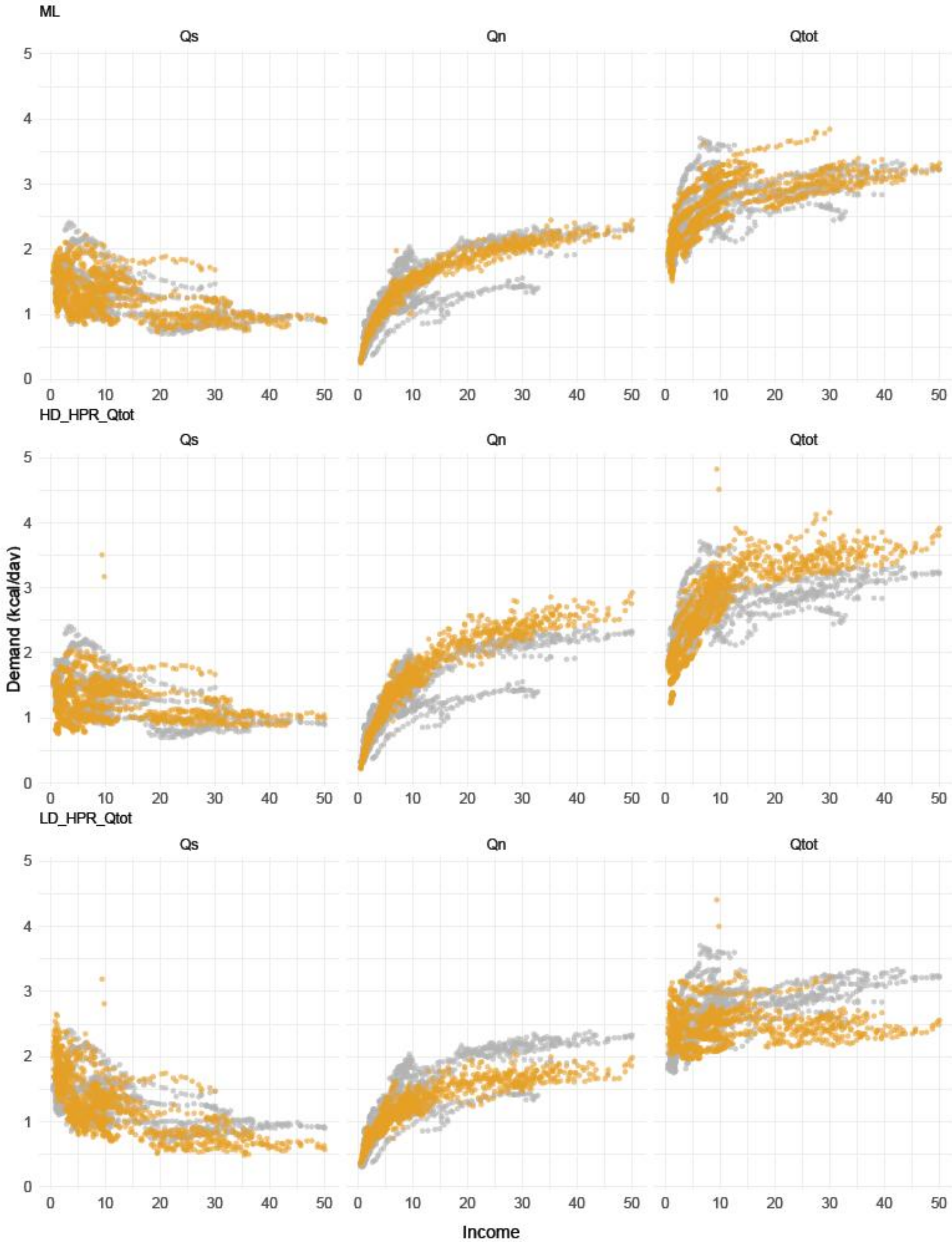

https://doi.org/10.5194/egusphere-2026-3848
Preprint. Discussion started: 21 July 2026

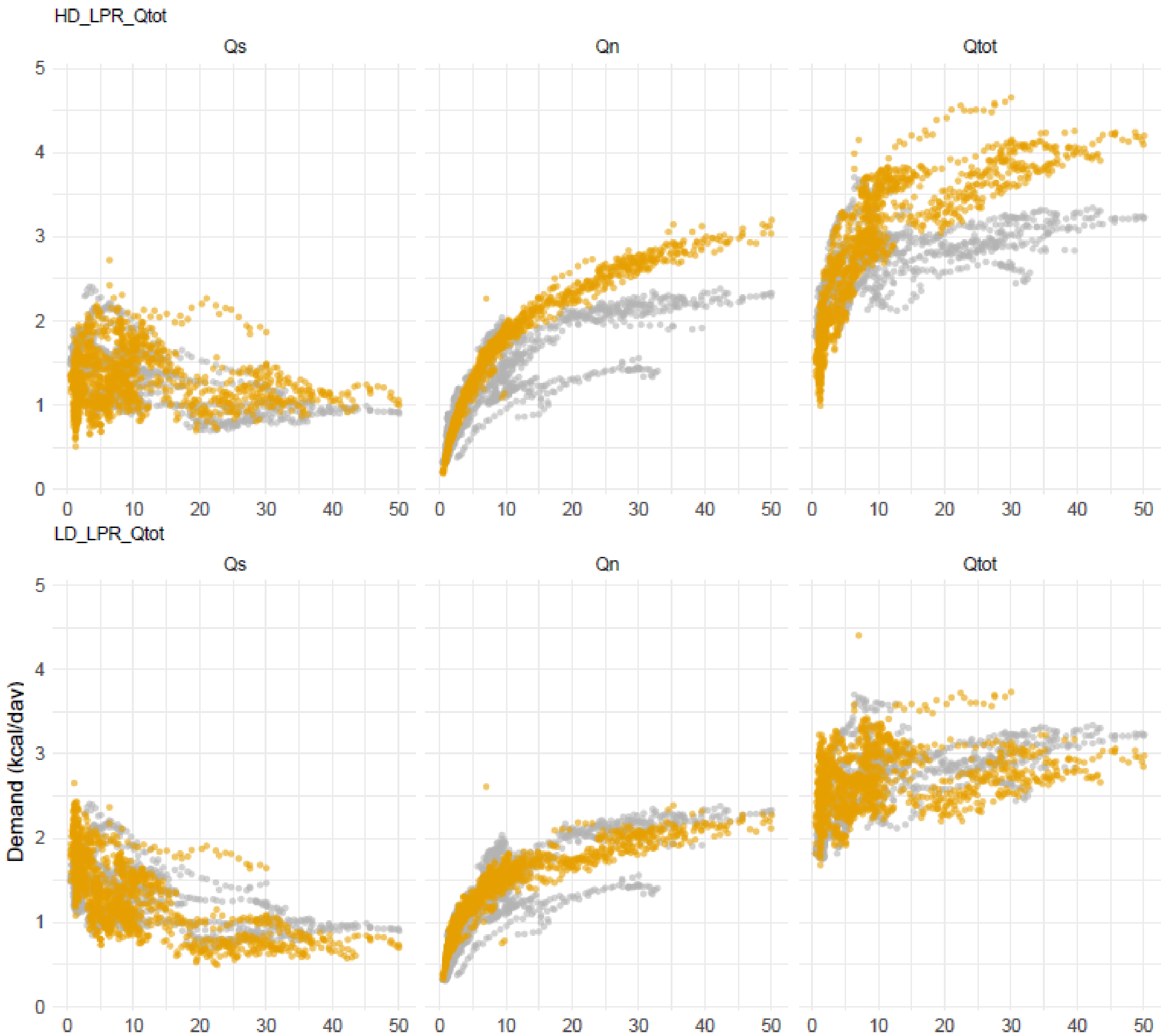

545 **B4. Uncertainty in demand for staples and non-staples**

Figure B5: Uncertainty in staples (a) and non-staples (b) demand in 2050 for GCAM regions. Bars span the 90% confidence interval. This supplements Figure 6 in the main text which shows results for total demand.

https://doi.org/10.5194/egusphere-2026-3848
Preprint. Discussion started: 21 July 2026

(a)

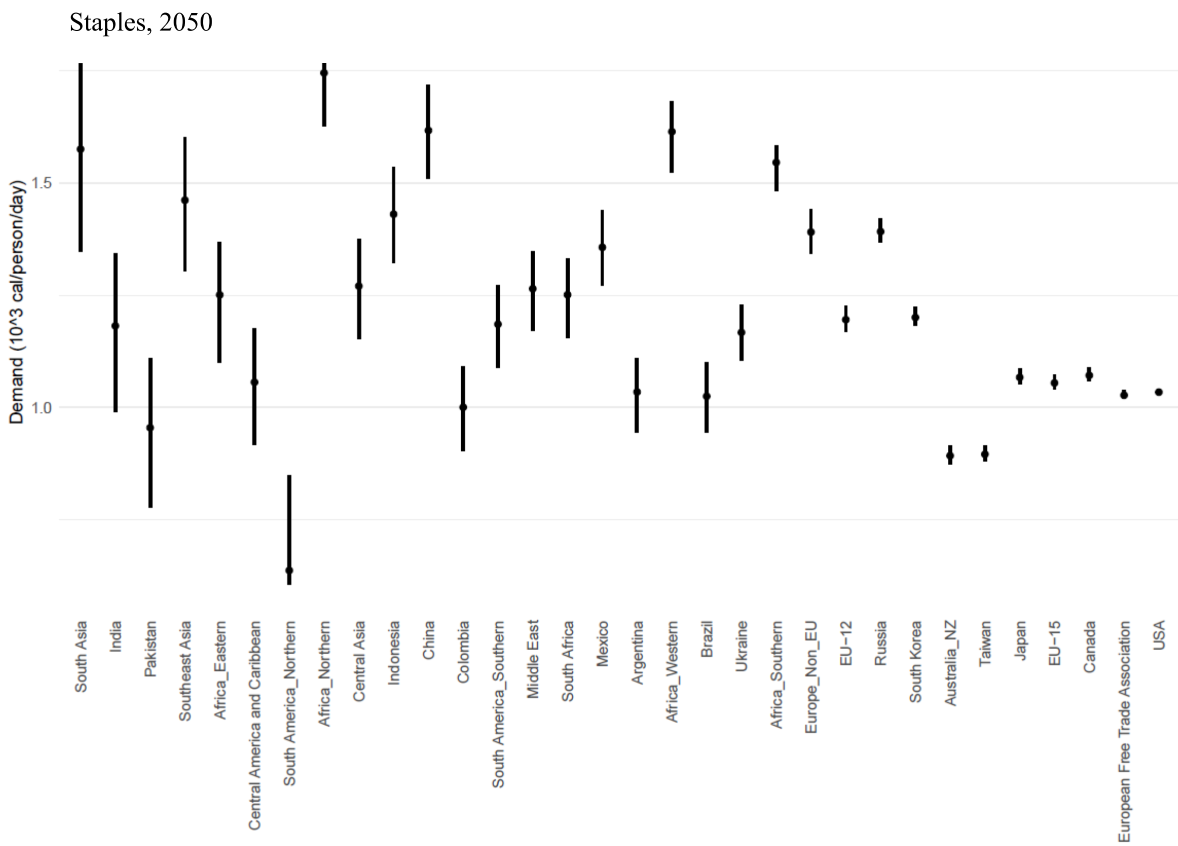

550

https://doi.org/10.5194/egusphere-2026-3848
Preprint. Discussion started: 21 July 2026

(b)

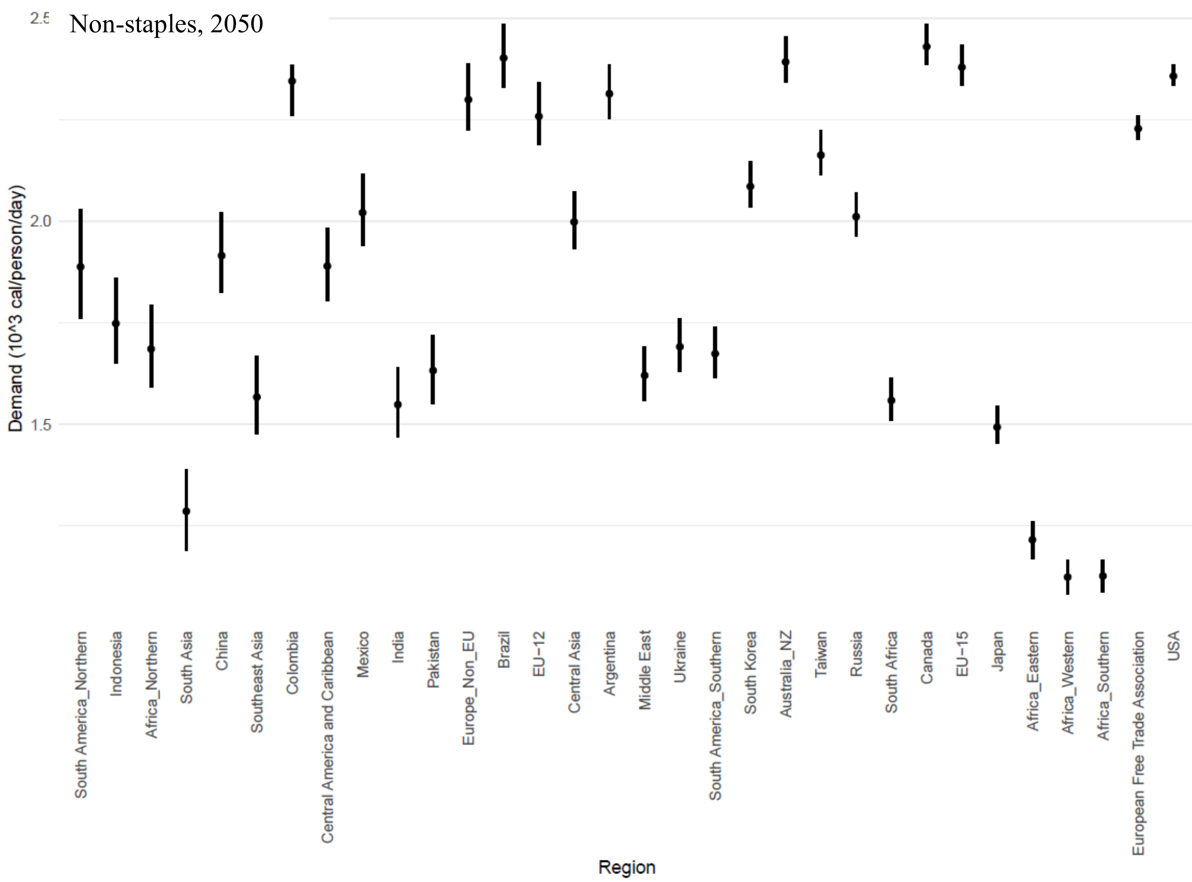

B5. Uncertainty in demand response to price change for staples and non-staples

Figure B6: Uncertainty in staples (a) and non-staples (b) demand difference between the High Price and Reference scenarios in 2050 for GCAM regions. Bars span the 90% confidence interval. This supplements Figure 9 in the main text which shows results for total demand.

https://doi.org/10.5194/egusphere-2026-3848
Preprint. Discussion started: 21 July 2026

(a)

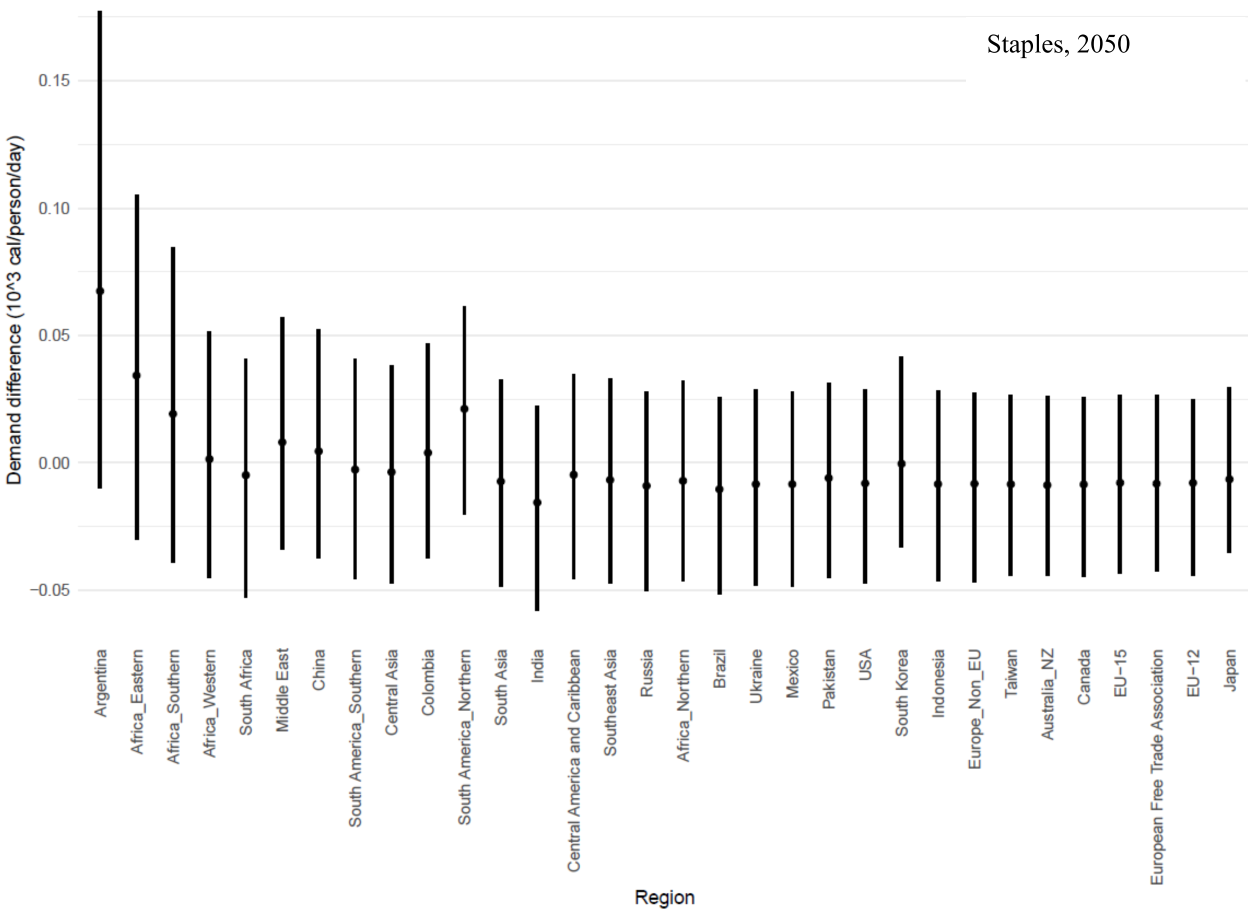

https://doi.org/10.5194/egusphere-2026-3848
Preprint. Discussion started: 21 July 2026

(b)

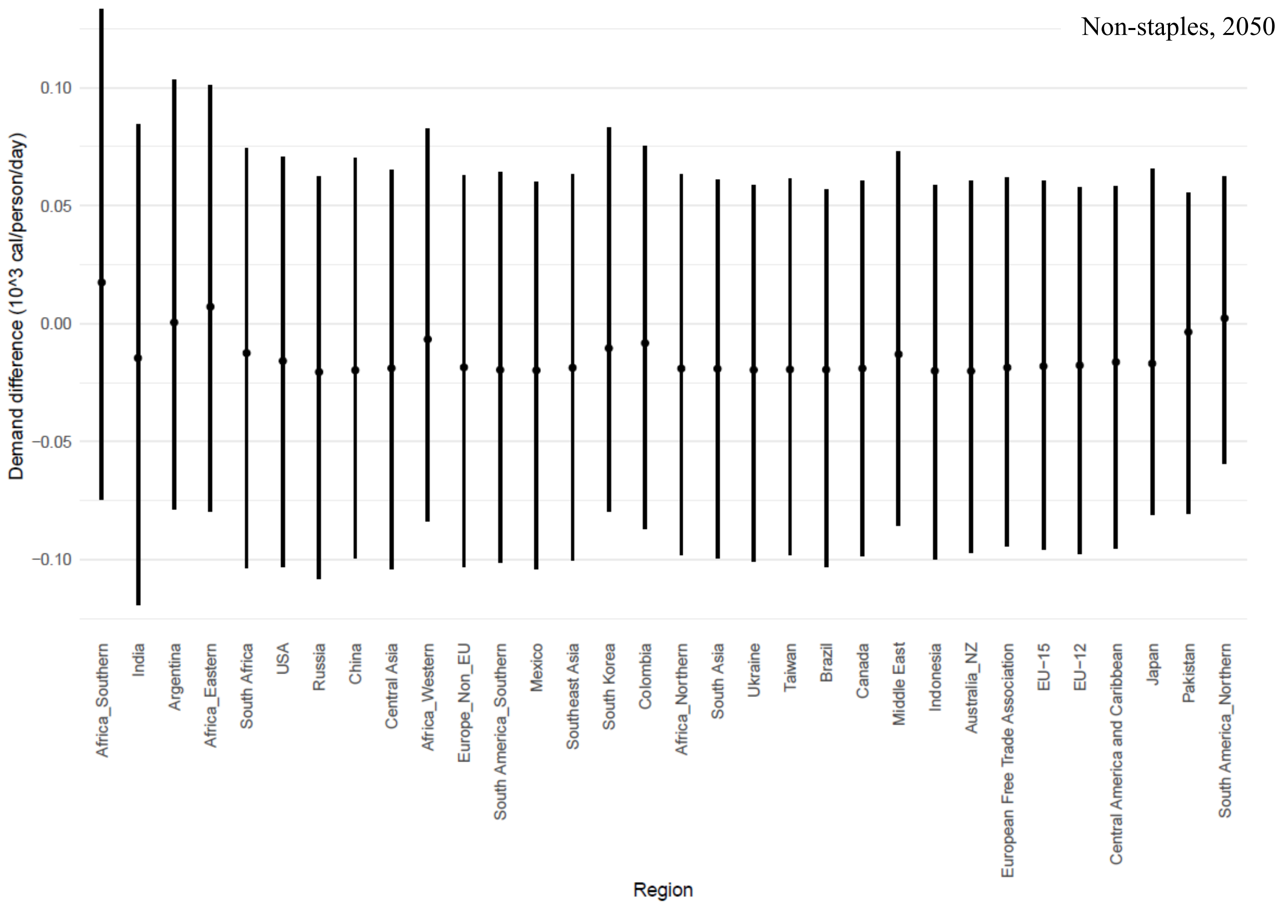

B6. ambrosia emulation of GCAM demand outcomes

Figure B7: Density distributions of differences between ambrosia vs GCAM staples and non-staples demand for all regions, five selected deciles, and all time periods for simulations with five different parameter sets. Panel (a) shows demand differences in the Reference scenario, panel (b) the High Price scenario, and panel (c) shows differences in the demand response to higher prices.

https://doi.org/10.5194/egusphere-2026-3848
Preprint. Discussion started: 21 July 2026

(a)

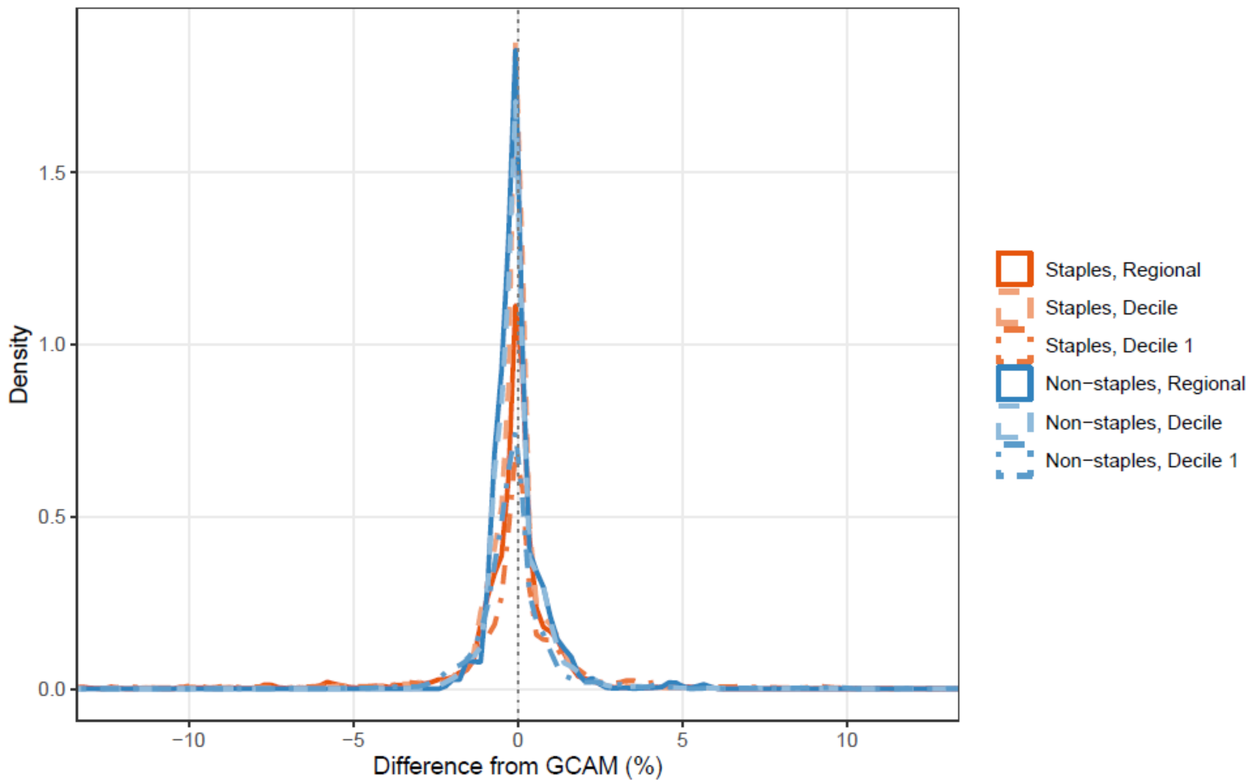

(b)

https://doi.org/10.5194/egusphere-2026-3848
Preprint. Discussion started: 21 July 2026

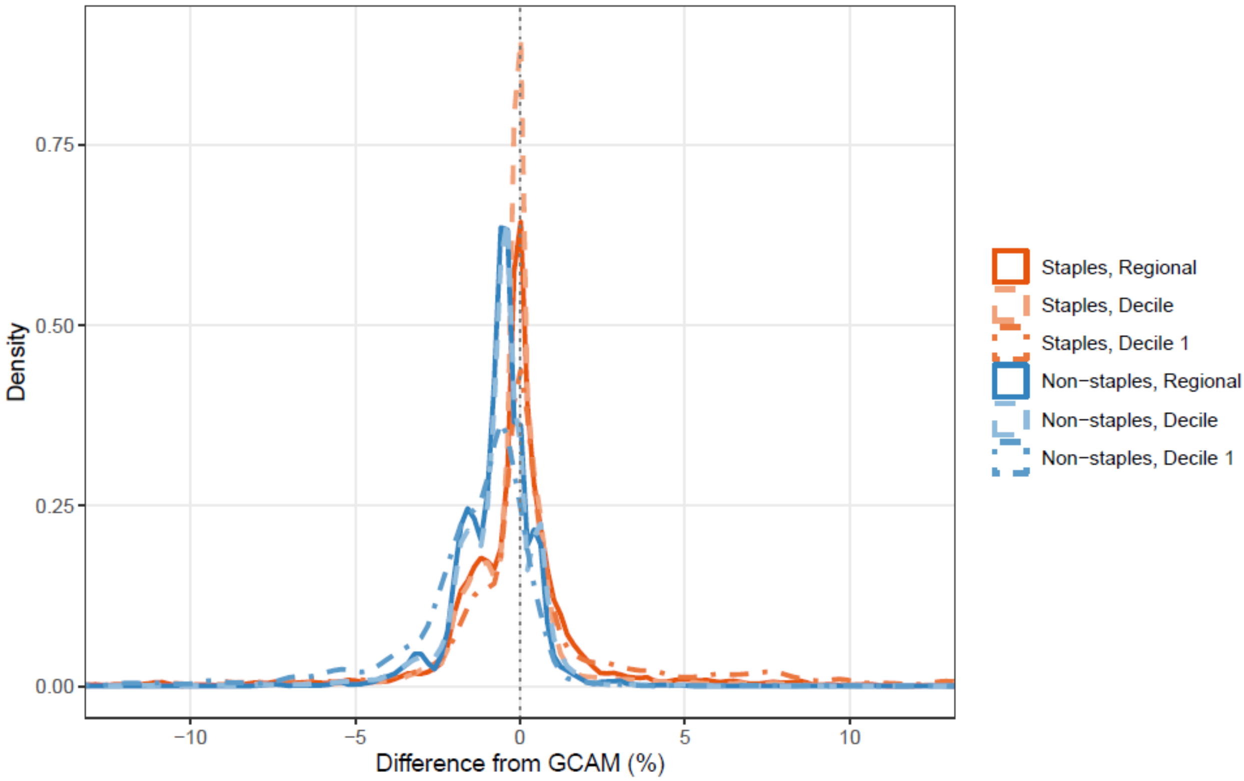

(c)

https://doi.org/10.5194/egusphere-2026-3848
Preprint. Discussion started: 21 July 2026

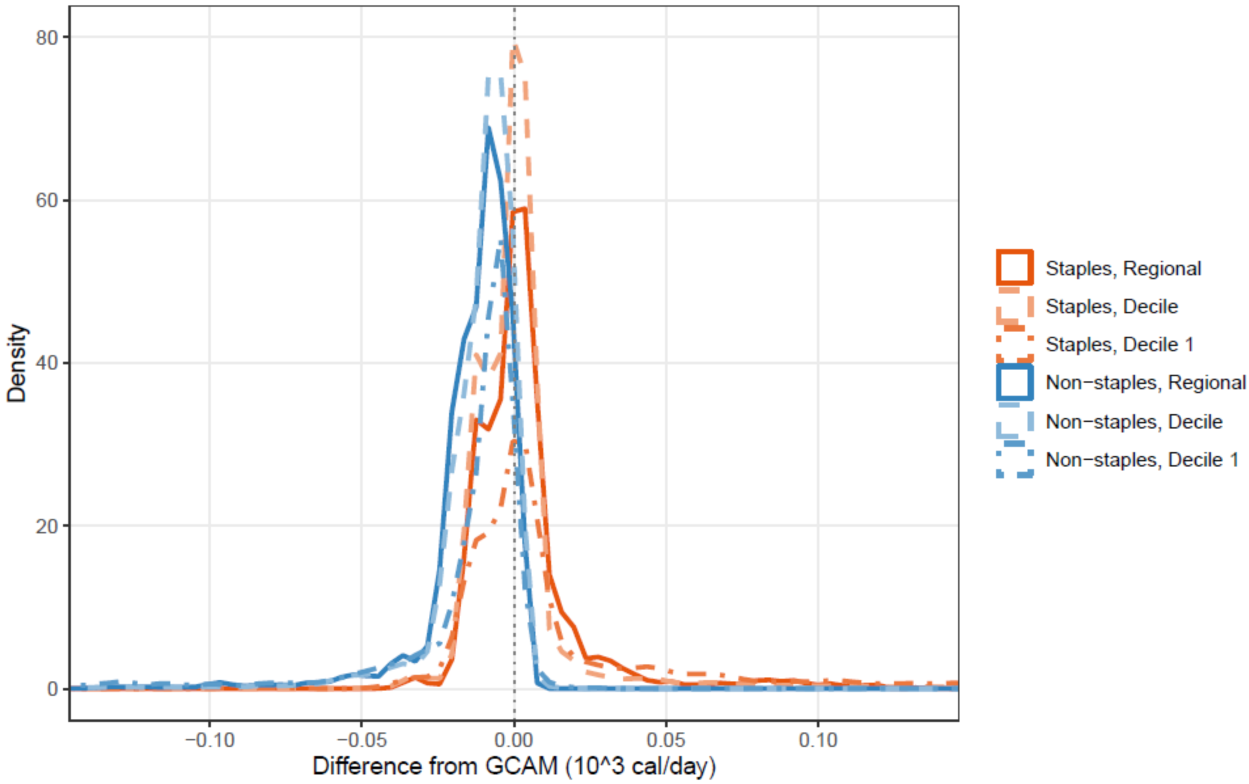

580

B7. Price difference in High Price Condition scenario relative to Reference scenario

Figure B8: Per capita income and prices of staples and non-staples for selected regions in the GCAM Reference and High Price scenarios.

https://doi.org/10.5194/egusphere-2026-3848
Preprint. Discussion started: 21 July 2026

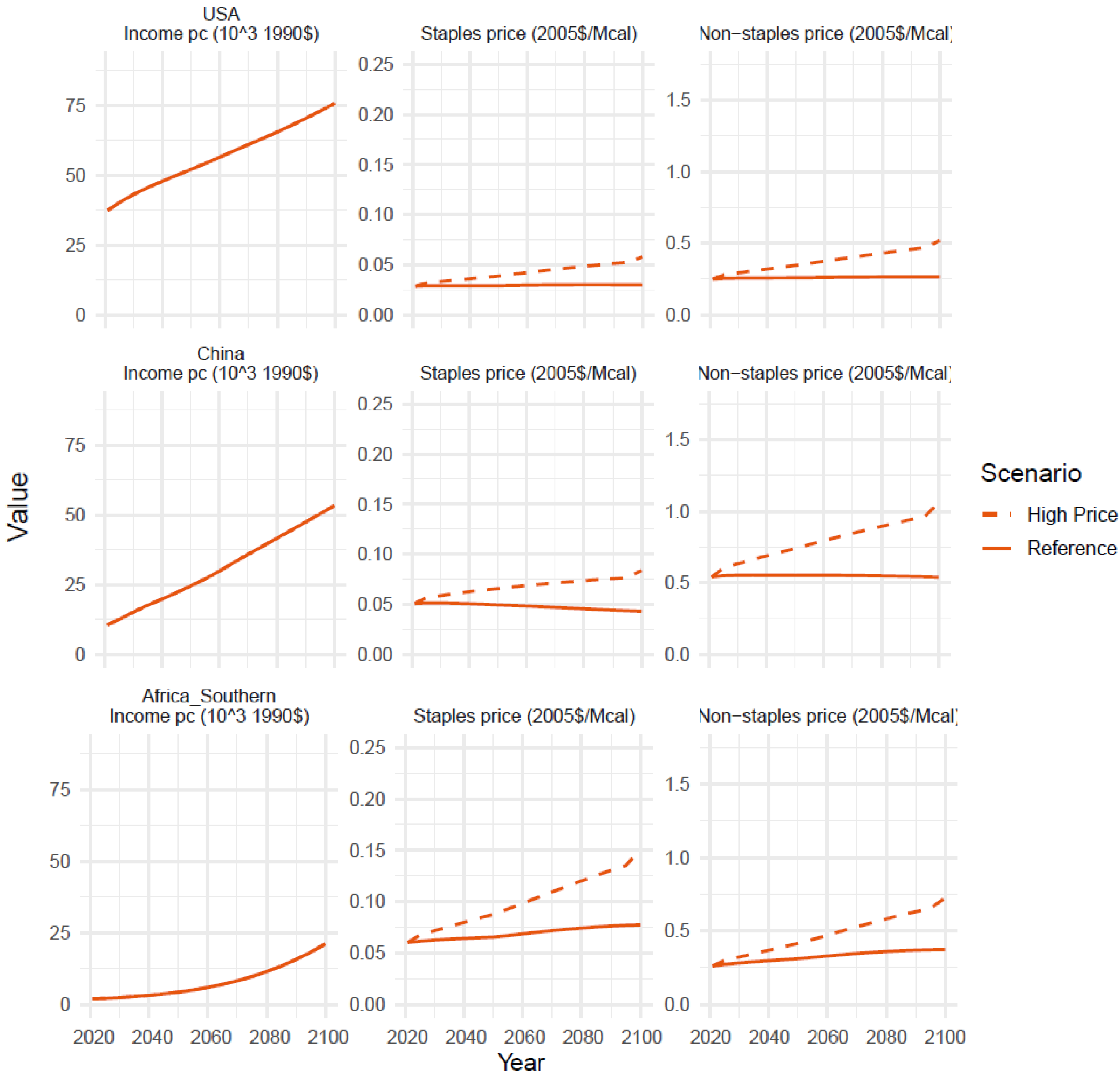

585

https://doi.org/10.5194/egusphere-2026-3848
Preprint. Discussion started: 21 July 2026

1.1.1. Appendix C

Appendix C contains additional tables.

C1. Prior distributions for demand function parameters

Table C1: Constraints on food demand parameters for the MCMC estimation.

Parameter	Minimum	Maximum
As	0	Inf
An	0	Inf
g.ss	-Inf	0
g.cross	-Inf	Inf
g.nn	-Inf	0
nu	0	Inf
lambda	0	Inf
kappa	1e-8	Inf
Pm	1e-6	Inf

C2. Goodness of fit metrics

Table C2: Goodness of fit metrics for GCAM vs historical observations of food demand, for the five different parameter sets identified in this study as well as the maximum likelihood parameters from Edmonds et al. (2017) (indicated by "ML 2017").

Parameters	**Demand type**	**N**	**RMSE**	**MAE**	**MAPE**	**Bias**	**Correlation (Pearson)**
ML	Staples	1264	0.148	0.111	8.442	-0.019	0.9
ML	Non-staples	1264	0.242	0.184	16.843	0.022	0.902
ML	Total	1264	0.278	0.215	8.356	0.002	0.807

https://doi.org/10.5194/egusphere-2026-3848
Preprint. Discussion started: 21 July 2026

HD-HPR	Staples	1264	0.22	0.167	12.755	-0.069	0.787
HD-HPR	Non-staples	1264	0.323	0.249	21.33	0.136	0.903
HD-HPR	Total	1264	0.421	0.336	13.145	0.067	0.807
HD-LPR	Staples	1264	0.256	0.207	16.178	-0.016	0.713
HD-LPR	Non-staples	1264	0.443	0.336	26.99	0.257	0.898
HD-LPR	Total	1264	0.591	0.462	17.691	0.241	0.817
LD-HPR	Staples	1264	0.264	0.207	16.134	-0.004	0.824
LD-HPR	Non-staples	1264	0.301	0.242	19.236	-0.136	0.892
LD-HPR	Total	1264	0.438	0.361	13.83	-0.14	0.352
LD-LPR	Staples	1264	0.248	0.194	14.952	0.012	0.832
LD-LPR	Non-staples	1264	0.273	0.215	20.627	0.066	0.878
LD-LPR	Total	1264	0.403	0.334	13.231	0.078	0.495
ML 2017	Staples	1264	0.287	0.233	18.045	-0.012	0.53
ML 2017	Non-staples	1264	0.241	0.186	16.864	0.013	0.901
ML 2017	Total	1264	0.293	0.217	8.296	0.002	0.734

https://doi.org/10.5194/egusphere-2026-3848
Preprint. Discussion started: 21 July 2026

C3. Identification of demand function parameter sets

Table C3: Numbers of region-time step groups that candidate parameter sets appear in. “Max. iteration” indicates the ID number of the iteration that appeared in the maximum number of groups. “Freq.” indicates the frequency with which that iteration appeared in the groups. Results for a given GCAM region show the iteration that works best for that region. Results for region 33 show global results, i.e., the iteration that works best across all regions.

	HD-HPR		**HD-LPR**		**LD-HPR**		**LD-LPR**	
GCAM region	**Max. iteration**	**Freq.**	**Max. iteration**	**Freq.**	**Max. iteration**	**Freq.**	**Max. iteration**	**Freq.**
1	75767	16	89453	15	105648	13	69500	16
2	71826	16	143147	12	111149	12	81994	16
3	78050	16	79058	16	111149	16	71534	16
4	74387	16	127223	9	140424	12	69500	16
5	71826	16	143147	14	69688	15	78629	16
6	75767	16	89453	16	140202	15	69500	16
7	85696	16	86055	16	140202	16	71534	16
8	75767	16	85060	15	101557	13	69500	16
9	77245	16	88408	16	90637	16	86178	16
10	78050	16	71430	16	85254	16	78629	16
11	85696	16	75934	16	72654	16	148516	16
12	75767	16	74097	16	111149	16	69500	16

https://doi.org/10.5194/egusphere-2026-3848
Preprint. Discussion started: 21 July 2026

13	75767	16	89453	16	111149	14	69500	16
14	85696	14	74097	14	111149	14	71534	14
15	78050	16	79058	16	105648	16	69500	16
16	75767	16	116356	16	140202	4	69500	16
17	78050	16	75934	16	85254	16	71534	16
18	78050	16	74097	16	75511	16	78629	16
19	75767	16	116356	15	105648	15	69500	16
20	78050	16	74097	16	90637	16	71534	16
21	85696	16	79058	16	105648	16	71534	16
22	77245	16	75934	15	90637	15	81994	13
23	150000	16	72847	15	75073	15	69500	16
24	78050	16	75934	16	74009	16	90175	16
25	127778	16	71430	16	101557	16	81994	12
26	85696	16	79058	16	105648	16	78629	16
27	78050	16	143147	16	114359	16	78629	16
28	77213	16	143147	16	105648	15	69500	16
29	78050	16	75934	16	74009	16	78629	16
30	75767	16	75205	16	101557	16	69500	16

https://doi.org/10.5194/egusphere-2026-3848
Preprint. Discussion started: 21 July 2026

31	89557	16	79058	15	75511	15	148516	12
32	77245	16	74097	16	75073	16	86178	16
33	138807	507	143147	489	140202	447	148516	475

Table C4: Global (a) and regional fixed effect (b) parameter values for the five scenarios identified in the main text.

(a)

Parameter	**ML**	**HD-HPR**	**HD-LPR**	**LD-HPR**	**LD-LPR**
As	1.209224	1.239717	1.129345	1.215833	1.172464
An	1.133505	1.244834	1.24542	1.101496	1.149135
g.ss	-0.16939	-0.09704	-0.32415	-0.24469	-0.24552
g.cross	0.136199	0.233054	0.09483	0.28333	0.061128
g.nn	-0.23429	-0.19262	-0.21882	-0.21209	-0.34046
nu	0.48958	0.572907	0.604283	0.397172	0.400265
lambda	0.097713	0.043657	0.032034	0.205146	0.173722
kappa	15.99872	16.07517	16.00388	16.01876	15.99563
Pm	4.967935	4.993638	5.001337	4.907093	4.979852

(b)

Region	**ML**	**HD-HPR**	**HD-LPR**	**LD-HPR**	**LD-LPR**
USA	-0.18596	-0.21818	-0.19409	-0.22411	-0.26321
Africa_Eastern	-0.38029	-0.48842	-0.3865	-0.41005	-0.44372
Africa_Northern	0.465929	0.502597	0.515494	0.487507	0.433194
Africa_Southern	0.044543	0.057816	-0.02421	0.085797	-0.06686
Africa_Western	0.03636	0.077432	0.021121	-0.01487	0.094504
Australia_NZ	-0.24284	-0.22181	-0.23516	-0.29032	-0.25443
Brazil	-0.01846	-0.12273	0.019362	0.018366	-0.00057

https://doi.org/10.5194/egusphere-2026-3848
Preprint. Discussion started: 21 July 2026

Canada	-0.04096	-0.05969	-0.0006	-0.00808	-0.07744
Central America and Caribbean	-0.33672	-0.37143	-0.41473	-0.29283	-0.34123
Central Asia	0.202239	0.244126	0.173605	0.263679	0.154182
China	0.256621	0.296511	0.222022	0.324859	0.229904
EU-12	0.226939	0.232695	0.236295	0.218837	0.113488
EU-15	-0.10392	-0.15536	-0.08569	-0.09148	-0.18305
Europe_Eastern	0.171876	0.161798	0.210043	0.153926	0.034779
Europe_Non_EU	0.661527	0.540233	0.687762	0.685914	0.648689
European Free Trade Association	-0.09128	-0.08479	-0.10295	-0.17051	-0.1188
India	-0.23952	-0.1561	-0.30507	-0.28239	-0.24163
Indonesia	0.170716	0.209129	0.188755	0.147112	0.1846
Japan	0.122173	0.130055	0.062148	0.145014	0.044279
Mexico	0.219484	0.28377	0.217267	0.233529	0.264029
Middle East	0.41042	0.347702	0.428668	0.376601	0.389494
Pakistan	-0.21062	-0.23801	-0.25636	-0.17367	-0.14293
Russia	0.271878	0.240781	0.305072	0.254886	0.230775
South Africa	0.438364	0.444078	0.421659	0.411622	0.417843
South America_Northern	-0.18963	-0.2172	-0.17867	-0.20463	-0.14314
South America_Southern	0.032585	0.000568	-0.01021	0.041856	0.110601
South Asia	0.046709	0.010741	0.02774	-0.03399	0.110018
South Korea	0.655772	0.569132	0.670084	0.648475	0.736432
Southeast Asia	-0.09833	-0.12951	-0.07642	-0.14621	-0.06422
Taiwan	0	0	0	0	0
Argentina	0.032317	-0.00798	-0.01012	-0.0209	-0.03544
Colombia	-0.17694	-0.16917	-0.20644	-0.20283	-0.24416

https://doi.org/10.5194/egusphere-2026-3848
Preprint. Discussion started: 21 July 2026

C4. Model comparison metrics

Table C5: Model comparison metrics for absolute demand as projected by ambrosia vs GCAM, for the Reference scenario.

Parameters	**Demand type**	**Decile**	**N**	**RMSE**	**MAE**	**Bias**	**Correlation (Pearson)**
ML	Staples	1	544	0.084	0.032	-0.018	0.964
ML	Staples	All	5440	0.035	0.009	-0.006	0.992
ML	Staples	Region	544	0.023	0.008	-0.006	0.996
ML	Non-staples	1	544	0.014	0.007	-0.001	1
ML	Non-staples	All	5440	0.009	0.005	-0.001	1
ML	Non-staples	Region	544	0.008	0.004	-0.001	1
ML	Total	1	544	0.074	0.029	-0.018	0.987
ML	Total	All	5440	0.029	0.009	-0.007	0.998
ML	Total	Region	544	0.017	0.008	-0.007	0.999
HD-HPR	Staples	1	544	0.109	0.038	-0.019	0.922
HD-HPR	Staples	All	5440	0.054	0.014	-0.008	0.98
HD-HPR	Staples	Region	544	0.043	0.013	-0.008	0.988
HD-HPR	Non-staples	1	544	0.02	0.01	-0.003	0.999
HD-HPR	Non-staples	All	5440	0.017	0.01	-0.005	1
HD-HPR	Non-staples	Region	544	0.015	0.01	-0.005	1

https://doi.org/10.5194/egusphere-2026-3848
Preprint. Discussion started: 21 July 2026

HD-HPR	Total	1	544	0.097	0.036	-0.022	0.982
HD-HPR	Total	All	5440	0.045	0.016	-0.012	0.998
HD-HPR	Total	Region	544	0.035	0.015	-0.012	0.997
HD-LPR	Staples	1	544	0.03	0.017	0.002	0.993
HD-LPR	Staples	All	5440	0.017	0.01	0.004	0.998
HD-LPR	Staples	Region	544	0.014	0.01	0.004	0.999
HD-LPR	Non-staples	1	544	0.007	0.003	0.001	1
HD-LPR	Non-staples	All	5440	0.008	0.004	0.002	1
HD-LPR	Non-staples	Region	544	0.007	0.004	0.002	1
HD-LPR	Total	1	544	0.026	0.016	0.003	0.999
HD-LPR	Total	All	5440	0.015	0.011	0.006	1
HD-LPR	Total	Region	544	0.013	0.01	0.006	1
LD-HPR	Staples	1	544	0.211	0.08	-0.03	0.903
LD-HPR	Staples	All	5440	0.077	0.018	-0.008	0.976
LD-HPR	Staples	Region	544	0.042	0.016	-0.008	0.987
LD-HPR	Non-staples	1	544	0.062	0.027	0.018	0.992
LD-HPR	Non-staples	All	5440	0.034	0.019	0.017	0.998
LD-HPR	Non-staples	Region	544	0.028	0.017	0.017	0.999

https://doi.org/10.5194/egusphere-2026-3848
Preprint. Discussion started: 21 July 2026

LD-HPR	Total	1	544	0.164	0.07	-0.012	0.952
LD-HPR	Total	All	5440	0.06	0.023	0.009	0.989
LD-HPR	Total	Region	544	0.029	0.019	0.009	0.997
LD-LPR	Staples	1	544	0.043	0.022	-0.02	0.995
LD-LPR	Staples	All	5440	0.019	0.011	-0.011	0.999
LD-LPR	Staples	Region	544	0.014	0.011	-0.011	0.999
LD-LPR	Non-staples	1	544	0.013	0.011	-0.009	1
LD-LPR	Non-staples	All	5440	0.015	0.013	-0.012	1
LD-LPR	Non-staples	Region	544	0.015	0.013	-0.012	1
LD-LPR	Total	1	544	0.044	0.029	-0.029	0.997
LD-LPR	Total	All	5440	0.028	0.024	-0.023	0.999
LD-LPR	Total	Region	544	0.026	0.023	-0.023	1

Table C6: Model comparison metrics for differences in demand due to price change (HP vs Reference scenario) as projected by ambrosia vs GCAM.

Parameters	**Demand type**	**Decile**	**N**	**RMSE**	**MAE**	**Bias**	**Correlation (Pearson)**
ML	Staples	1	544	0.055	0.025	0.023	0.651
ML	Staples	All	5440	0.021	0.006	0.004	0.651
ML	Staples	Region	544	0.012	0.005	0.004	0.67

https://doi.org/10.5194/egusphere-2026-3848
Preprint. Discussion started: 21 July 2026

ML	Non-staples	1	544	0.029	0.016	-0.016	0.793
ML	Non-staples	All	5440	0.015	0.01	-0.01	0.966
ML	Non-staples	Region	544	0.012	0.01	-0.01	0.986
ML	Total	1	544	0.032	0.017	0.007	0.899
ML	Total	All	5440	0.015	0.01	-0.006	0.971
ML	Total	Region	544	0.01	0.008	-0.006	0.988
HD-HPR	Staples	1	544	0.123	0.055	0.054	0.612
HD-HPR	Staples	All	5440	0.051	0.018	0.018	0.662
HD-HPR	Staples	Region	544	0.034	0.018	0.018	0.803
HD-HPR	Non-staples	1	544	0.109	0.04	-0.039	-0.675
HD-HPR	Non-staples	All	5440	0.048	0.015	-0.014	0.048
HD-HPR	Non-staples	Region	544	0.031	0.014	-0.014	0.251
HD-HPR	Total	1	544	0.057	0.027	0.015	0.868
HD-HPR	Total	All	5440	0.024	0.009	0.003	0.924
HD-HPR	Total	Region	544	0.015	0.009	0.003	0.961
HD-LPR	Staples	1	544	0.024	0.018	-0.004	0.88
HD-LPR	Staples	All	5440	0.016	0.014	-0.011	0.969
HD-LPR	Staples	Region	544	0.014	0.012	-0.011	0.984

https://doi.org/10.5194/egusphere-2026-3848
Preprint. Discussion started: 21 July 2026

HD-LPR	Non-staples	1	544	0.024	0.015	-0.015	0.949
HD-LPR	Non-staples	All	5440	0.017	0.013	-0.013	0.989
HD-LPR	Non-staples	Region	544	0.016	0.013	-0.013	0.993
HD-LPR	Total	1	544	0.025	0.021	-0.019	0.99
HD-LPR	Total	All	5440	0.028	0.025	-0.024	0.995
HD-LPR	Total	Region	544	0.027	0.024	-0.024	0.996
LD-HPR	Staples	1	544	0.173	0.078	0.074	0.67
LD-HPR	Staples	All	5440	0.065	0.017	0.016	0.731
LD-HPR	Staples	Region	544	0.035	0.016	0.016	0.73
LD-HPR	Non-staples	1	544	0.097	0.037	-0.036	-0.354
LD-HPR	Non-staples	All	5440	0.036	0.009	-0.008	0.381
LD-HPR	Non-staples	Region	544	0.019	0.009	-0.008	0.733
LD-HPR	Total	1	544	0.119	0.053	0.038	0.772
LD-HPR	Total	All	5440	0.043	0.012	0.008	0.816
LD-HPR	Total	Region	544	0.022	0.011	0.008	0.866
LD-LPR	Staples	1	544	0.022	0.014	0.001	0.912
LD-LPR	Staples	All	5440	0.011	0.008	-0.005	0.957
LD-LPR	Staples	Region	544	0.008	0.007	-0.005	0.98

https://doi.org/10.5194/egusphere-2026-3848
Preprint. Discussion started: 21 July 2026

LD-LPR	Non-staples	1	544	0.021	0.018	-0.018	0.993
LD-LPR	Non-staples	All	5440	0.022	0.02	-0.02	0.996
LD-LPR	Non-staples	Region	544	0.022	0.02	-0.02	0.996
LD-LPR	Total	1	544	0.026	0.022	-0.017	0.986
LD-LPR	Total	All	5440	0.029	0.026	-0.025	0.994
LD-LPR	Total	Region	544	0.028	0.025	-0.025	0.995

5. Code and data availability

The version of GCAM used for producing scenarios for this analysis, along with code for the MCMC parameter estimation, is preserved at https://zenodo.org/records/15085110. Version 2 of ambrosia used for generating ensembles of food demand projections is available at https://zenodo.org/records/15085110 (Narayan et al., 2021). The code used for generating and analyzing ambrosia simulations, as well as for generating all figures and tables, is available at Zenodo via https://doi.org/10.5281/zenodo.20450340 with Open Access (O'Neill, 2026).

6. Author contributions

All authors conceptualized the analysis and paper. BCO and KN carried out the formal analysis. BCO led the writing of the paper; all authors contributed to the original draft, reviewing, and editing.

7. Competing interests

The authors declare there are no competing interests for this manuscript

8. Financial support

This research was supported by the U.S. Department of Energy, Office of Science, as part of research in MultiSector Dynamics, Earth and Environmental System Modeling Program. The Pacific Northwest National Laboratory is operated for DOE by Battelle Memorial Institute under contract DE-AC05-76RL01830. The views and opinions expressed in this paper are those of the authors alone.

https://doi.org/10.5194/egusphere-2026-3848
Preprint. Discussion started: 21 July 2026

9. References

Andreyeva, T., Long, M. W., and Brownell, K. D. : The impact of food prices on consumption: A systematic review of research on the price elasticity of demand for food. American Journal of Public Health, 100(2), 216–222. https://doi.org/10.2105/AJPH.2008.151415, 2010.

Bijl, D. L., Bogaart, P. W., Dekker, S. C., Stehfest, E., de Vries, B. J. M., and van Vuuren, D. P. : A physically-based model of long-term food demand. Global Environmental Change, 45, 47–62. https://doi.org/10.1016/j.gloenvcha.2017.04.003, 2017.

Binsted, M., Iyer, G., Patel, P., Graham, N., Ou, Y., Khan, Z., Kholod, N., Narayan, K., Hejazi, M., Kim, S., and Calvin, K. : GCAM-USA v5.3_water_dispatch: integrated modeling of subnational US energy, water, and land systems within a global framework. Geoscientific Model Development, 14(10), 6465–6488. https://doi.org/10.5194/gmd-14-6465-2021, 2021.

Blundell, R., and Stoker, T. M. : Heterogeneity and aggregation. Journal of Economic Literature, 43(2), 347–391. https://doi.org/10.1257/0022051054661486, 2005.

Bodirsky, B., Rolinski, S., Biewald, A., Weindl, I., Popp, A., and Lotze-Campen, H. : Global food demand scenarios for the 21st century. PLoS ONE, 10(11), e0139201. https://doi.org/10.1371/journal.pone.0139201, 2015.

Calvin, K., Patel, P., Clarke, L., Asrar, G., Bond-Lamberty, B., Cui, R. Y., Di Vittorio, A., Dorheim, K., Edmonds, J., Hartin, C., and Hejazi, M. : GCAM v5.1: representing the linkages between energy, water, land, climate, and economic systems. Geoscientific Model Development, 12(2), 677–698. https://doi.org/10.5194/gmd-12-677-2019, 2019.

Cirera, X., and Masset, E. : Income distribution trends and future food demand. Philosophical Transactions of the Royal Society B: Biological Sciences, 365(1554), 2821–2834. https://doi.org/10.1098/rstb.2010.0164, 2010.

Cranfield, J. A. L., Eales, J. S., Hertel, T. W., and Preckel, P. V. : Model selection when estimating and predicting consumer demands using international, cross section data. Empirical Economics, 28(2), 353–364. https://doi.org/10.1007/s001810200135, 2003.

Denton, F. T., and Mountain, D. C. : Income distribution and aggregation/disaggregation biases in the measurement of consumer demand elasticities. Economics Letters, 73(1), 21–28. https://doi.org/10.1016/S0165-1765(01)00461-X, 2001.

Denton, F. T., and Mountain, D. C. : Exploring the effects of aggregation error in the estimation of consumer demand elasticities. Economic Modelling, 28(4), 1747–1755. https://doi.org/10.1016/j.econmod.2011.03.010, 2011.

Edmonds, J. A., Link, R., Waldhoff, S. T., and Cui, R. : A global food demand model for the assessment of complex human-earth systems. Climate Change Economics, 8(4), 1750012. https://doi.org/10.1142/S2010007817500129, 2017.

Flies, E. J., Brook, B. W., Blomqvist, L., and Buettel, J. C. : Forecasting future global food demand: A systematic review and meta-analysis of model complexity. Environment International, 120, 93–103. https://doi.org/10.1016/j.envint.2018.07.019, 2018.

Franke, J. A., Müller, C., Elliott, J., Ruane, A. C., Jägermeyr, J., Snyder, A., Dury, M., Falloon, P. D., Folberth, C., François, L., Hank, T., Izaurralde, R. C., Jacquemin, I., Jones, C., Li, M., Liu, W., Olin, S., Phillips, M., Pugh, T. A. M., and Moyer, E.

J. : The GGCMI Phase 2 emulators: global gridded crop model responses to changes in CO2, temperature, water, and nitrogen (version 1.0). Geoscientific Model Development, 13(9), 3995–4018. https://doi.org/10.5194/gmd-13-3995-2020, 2020.

Hertel, T. W. (Ed.). : Global trade analysis: Modeling and applications. Cambridge University Press, 1997.

Holmes, A., Jensen, M., Coffland, S., Shen, H. M., Sizemore, L., Bassetti, S., Nieva, B., Tebaldi, C., Snyder, A., and Hutchinson, B. : Emulating the Global Change Analysis Model with deep learning. In Proceedings of the AAAI Conference on Artificial Intelligence, 2024.

Joint Global Change Research Institute. : GCAM Wiki documentation. Retrieved from https://wiki.umd.edu/gcam/, 2025.

Kumar, P., Kumar, A., Parappurathu, S., and Raju, S. S. : Estimation of demand elasticity for food commodities in India. Agricultural Economics Research Review, 24, 1–14, 2011.

Lamontagne, J. R., Reed, P. M., Link, R., Calvin, K. V., Clarke, L. E., and Edmonds, J. A. : Large ensemble analytic framework for consequence-driven discovery of climate change scenarios. Earth's Future, 6(3), 488–504. https://doi.org/10.1002/2017EF000701, 2018.

Li, L., Zhai, S.-X., and Bai, J.-F. : The dynamic impact of income and income distribution on food consumption among adults in rural China. Journal of Integrative Agriculture, 20(1), 330–342. https://doi.org/10.1016/S2095-3119(20)63239-7, 2021.

Muhammad, A., Seale, J. L., Jr., Meade, B., and Regmi, A. : International evidence on food consumption patterns: An update using 2005 international comparison program data. USDA Economic Research Service Technical Bulletin No. 1929, 2011.

Narayan, K., Waldhoff, S. T., Edmonds, J. A., and Cui, R. : ambrosia: An R package for calculating and analyzing food demand that is responsive to changing incomes and prices. Journal of Open Source Software, 6(59), 2890. https://doi.org/10.21105/joss.02890, 2021.

Narayan, K. B., O'Neill, B. C., Waldhoff, S. T., and Tebaldi, C. : Non-parametric projections of national income distribution consistent with the Shared Socioeconomic Pathways. Environmental Research Letters, 18(4), 044013. https://doi.org/10.1088/1748-9326/acbdb0, 2023.

Nelson, G. C., van der Mensbrugghe, D., Ahammad, H., Blanc, E., Calvin, K. C., Hasegawa, T., Havlik, P., Heyhoe, E., Kyle, G. P., Lotze-Campen, H., von Lampe, M., Mason d'Croz, D., van Meijl, H., Müller, C., Reilly, J., Robertson, R., Sands, R., Schmitz, C., Tabeau, A., and Willenbockel, D. : Agriculture and climate change in global scenarios: Why don't the models agree? Agricultural Economics, 45(1), 85–101. https://doi.org/10.1111/agec.12091, 2014.

Nicholls, Z. R. J., Meinshausen, M., Lewis, J., Gieseke, R., Dommenget, D., Dorheim, K., Fan, C. S., Fuglestvedt, J. S., Gasser, T., Golüke, U., Goodwin, P., Hartin, C., Hope, A. P., Kriegler, E., Leach, N. J., Marchegiani, D., McBride, L. A., Quilcaille, Y., Rogelj, J., and Xie, Z. : Reduced Complexity Model Intercomparison Project Phase 1: introduction and evaluation of global-mean temperature response. Geoscientific Model Development, 13(11), 5175–5190. https://doi.org/10.5194/gmd-13-5175-2020, 2020.

O'Neill, B.C. (2026). Earth's Future "Quantifying parametric uncertainty in future food demand" – Data and software [Dataset]. Zenodo. https://zenodo.org/records/20450656

O'Neill, B., Kriegler, E., Riahi, K., Ebi, K., Hallegatte, S., Carter, T., Mathur, R., and van Vuuren, D. : A new scenario framework for climate change research: the concept of shared socioeconomic pathways. Climatic Change, 122(3), 387–400. https://doi.org/10.1007/s10584-013-0905-2, 2014.

O'Neill, B. C., Jiang, L., KC, S., Fuchs, R., Pachauri, S., Laidlaw, E. K., Zhang, T., Zhou, W., and Ren, X. : The effect of education on determinants of climate change risks. Nature Sustainability, 3(7), 520–528. https://doi.org/10.1038/s41893-020-0512-y, 2020.

Park, J. L., Holcomb, R. B., Raper, K. C., and Capps, O., Jr. : A demand systems analysis of food commodities by U.S. households segmented by income. American Journal of Agricultural Economics, 78(2), 290–300. https://doi.org/10.2307/1243703, 1996.

Pinstrup-Andersen, P., and Caicedo, E. : The potential impact of changes in income distribution on food demand and human nutrition. American Journal of Agricultural Economics, 60(3), 402–415. https://doi.org/10.2307/1239937, 1978.

Reilly, M., and Willenbockel, D. : Managing uncertainty: a review of food system scenario analysis and modelling. Philosophical Transactions of the Royal Society B: Biological Sciences, 365(1554), 3049–3063. https://doi.org/10.1098/rstb.2010.0141, 2010.

Ren, Y., Zhang, Y., Loy, J.-P., and Glauben, T. : Food consumption among income classes and its response to changes in income distribution in rural China. China Agricultural Economic Review, 10(3), 406–424. https://doi.org/10.1108/CAER-08-2014-0079, 2018.

Roche, M., Comstock, A., and Ecker, O. : The future of food demand: A global meta-analysis and projections of income and price elasticities (IFPRI Discussion Paper No. 2361), 2025.

Sampedro, J., Iyer, G., Msangi, S., Waldhoff, S., Hejazi, M., and Edmonds, J. A. : Implications of different income distributions for future residential energy demand in the U.S. Environmental Research Letters, 17(1), 014031. https://doi.org/10.1088/1748-9326/ac43df, 2022.

Sampedro, J., Waldhoff, S. T., Edmonds, J. A., Iyer, G., Msangi, S., Narayan, K. B., Patel, P., and Wise, M. : Residential energy demand, emissions, and expenditures at regional and income-decile level for alternative futures. Environmental Research Letters, 19(8), 084031. https://doi.org/10.1088/1748-9326/ad6015, 2024.

Snyder, A., Calvin, K. V., Phillips, M., and Ruane, A. C. : A crop yield change emulator for use in GCAM and similar models: Persephone v1.0. Geoscientific Model Development, 12(4), 1319–1350. https://doi.org/10.5194/gmd-12-1319-2019, 2019.

Tebaldi, C., Snyder, A., and Dorheim, K. : STITCHES: creating new scenarios of climate model output by stitching together pieces of existing simulations. Earth System Dynamics, 13(4), 1557–1609. https://doi.org/10.5194/esd-13-1557-2022, 2022.

Tiffin, A., and Tiffin, R. : Estimates of food demand elasticities for Great Britain: 1972–1994. Journal of Agricultural Economics, 50(1), 140–147. https://doi.org/10.1111/j.1477-9552.1999.tb00800.x, 1999.

https://doi.org/10.5194/egusphere-2026-3848
Preprint. Discussion started: 21 July 2026

Valin, H., Sands, R. D., van der Mensbrugghe, D., Nelson, G. C., Ahammad, H., Blanc, E., Bodirsky, B., Fujimori, S., Hasegawa, T., Havlik, P., Heyhoe, E., Kyle, P., Mason-D'Croz, D., Paltsev, S., Rolinski, S., Tabeau, A., van Meijl, H., von Lampe, M., and Willenbockel, D. : The future of food demand: understanding differences in global economic models. Agricultural Economics, 45(1), 51–67. https://doi.org/10.1111/agec.12089, 2014.

van Dijk, M., and Meijerink, G. W. : A review of global food security scenario and assessment studies: Results, gaps and research priorities. Global Food Security, 3(3), 227–238. https://doi.org/10.1016/j.gfs.2014.09.004, 2014.

van Dijk, M., Morley, T., Rau, M. L., and Saghai, Y. : A meta-analysis of projected global food demand and population at risk of hunger for the period 2010–2050. Nature Food, 2(7), 494–501. https://doi.org/10.1038/s43016-021-00322-9, 2021.

von Lampe, M., Willenbockel, D., Ahammad, H., Blanc, E., Cai, Y., Calvin, K., Fujimori, S., Hasegawa, T., Havlik, P., Heyhoe, E., Kyle, P., Lotze-Campen, H., Mason d'Croz, D., Nelson, G. C., Sands, R. D., Schmitz, C., Tabeau, A., Valin, H., van der Mensbrugghe, D., and van Meijl, H. : Why do global long-term scenarios for agriculture differ? An overview of the AgMIP Global Economic Model Intercomparison. Agricultural Economics, 45(1), 3–20. https://doi.org/10.1111/agec.12086, 2014.

Xiong, W., Tanaka, K., Ciais, P., Johansson, D. J. A., and Lehtveer, M. : emIAM v1.0: an emulator for integrated assessment models using marginal abatement cost curves. Geoscientific Model Development, 18(5), 1575–1612. https://doi.org/10.5194/gmd-18-1575-2025, 2025.

Yu, W., Hertel, T. W., Preckel, P. V., and Eales, J. S. : Projecting world food demand using alternative demand systems. Economic Modelling, 21(1), 99–129. https://doi.org/10.1016/S0264-9993(02)00086-X, 2004.

Zhang, Y., Ou, Y., Waldhoff, S., O'Neill, B., Iyer, G., Sampedro, J., and Casper, K. : Long-term decarbonization impacts on residential energy security across income groups and US states. Environmental Research Letters, 20(5), 054040. https://doi.org/10.1088/1748-9326/adca4c, 2025.

Zhao, X., Wise, M. A., Waldhoff, S. T., Kyle, G. P., Huster, J. E., Ramig, C. W., Rafelski, L. E., Patel, P. L., and Calvin, K. V. : The impact of agricultural trade approaches on global economic modeling. Global Environmental Change, 73, 102413. https://doi.org/10.1016/j.gloenvcha.2022.102413, 2022.